

STABLE TRAINING OF NORMALIZING FLOWS FOR HIGH-DIMENSIONAL VARIATIONAL INFERENCE

DANIEL ANDRADE

School of Informatics and Data Science, Hiroshima University

ABSTRACT. Variational inference with normalizing flows (NFs) is an increasingly popular alternative to MCMC methods. In particular, NFs based on coupling layers (Real NVPs) are frequently used due to their good empirical performance. In theory, increasing the depth of normalizing flows should lead to more accurate posterior approximations. However, in practice, training deep normalizing flows for approximating high-dimensional posterior distributions is often infeasible due to the high variance of the stochastic gradients. In this work, we show that previous methods for stabilizing the variance of stochastic gradient descent can be insufficient to achieve stable training of Real NVPs. As the source of the problem, we identify that, during training, samples often exhibit unusual high values. As a remedy, we propose a combination of two methods: (1) soft-thresholding of the scale in Real NVPs, and (2) a bijective soft log transformation of the samples. We evaluate these and other previously proposed modification on several challenging target distributions, including a high-dimensional horseshoe logistic regression model. Our experiments show that with our modifications, stable training of Real NVPs for posteriors with several thousand dimensions is possible, allowing for more accurate marginal likelihood estimation via importance sampling. Moreover, we evaluate several common training techniques and architecture choices and provide practical advice for training NFs for high-dimensional variational inference.

1. INTRODUCTION

During the past decade, variational inference (VI) has been gaining increased attention also in the statistics community [Blei et al., 2017]. Thanks to its computational efficiency, VI can provide useful approximations to high-dimensional posterior distributions that are computationally too expensive for MCMC methods. However, simple variational distributions, like the Gaussian distribution, can lead to arbitrarily bad approximations [Zhang et al., 2018].

As a promising method for increasing the expressibility of the VI approximation, normalizing flows (NFs) have been proposed [Papamakarios et al., 2021]. In particular, normalizing flows based on coupling layers (Real NVP) are known to have good performance for variational inference [Dhaka et al., 2021, Vaitl et al., 2022]. Real NVPs also have the advantage that both sampling and density estimation is computationally efficient, making them the optimal choice for importance sampling. Unfortunately, for high dimensional posterior distributions, VI with NFs is known to suffer from unstable training, and therefore most previous works limit

E-mail address: andrade@hiroshima-u.ac.jp.

their application to posteriors with less than hundred dimensions [Dhaka et al., 2021, Vaitl et al., 2022, Liang et al., 2022].

As one source of the unstable training, we identify that Real NVPs with increasing depth are prone to produce exponentially large sample values. This poses a dilemma, since an increase in depth is also known to increase the expressibility of the resulting posterior approximation [Koehler et al., 2021]. As a remedy, we propose to (1) soft-threshold the scaling in Real NVPs, and (2) to pass all samples through a bijective soft log transformation (named LOFT).¹ We demonstrate that with these modifications, the NFs’ samples that are used for gradient estimation can exhibit considerably lower variance, which consequently ensures good convergence even for high-dimensional target distributions with fat tails. In particular, for logistic regression with the horseshoe prior and more than 4000 dimensions we achieve significantly sharper estimates of the marginal likelihood than previous NFs and sequential Monte Carlo (SMC) [Dai et al., 2022]. Orthogonal to this work, we note that normalizing flows and SMC can be effectively combined to further improve the marginal likelihood estimate [Arbel et al., 2021, Matthews et al., 2022].

Furthermore, in this article, we also scrutinize and evaluate several other subtle modifications in the architecture and training of Real NVPs, like path gradients [Roeder et al., 2017] and annealing [Rezende and Mohamed, 2015]. Our analysis shows that some of these modifications can have a significant impact on approximation accuracy. We also empirically verify that for training NFs, the evidence lower bound (ELBO) is well suited as training objective due to its high correlation with the accuracy of the marginal likelihood estimate.

Behrmann et al. [2021] prove that Real NVPs are not globally Lipschitz continuous, which can lead to numerical instability of the inverse. As a remedy, Behrmann et al. [2021], Ardizzone et al. [2019] propose to restrict the output out of the scalings. However, their focus is on the inverse, in particular on the reconstruction of image data. As we show in Section 7, their proposed restrictions can be sub-optimal for training in variational inference. On the other hand, the works in [Salmona et al., 2022, Hagemann and Neumayer, 2021] show that multi-modal target distributions can lead to exploding Lipschitz constants, which can be mitigated by changing the base distribution to a multivariate normal mixture model. However, training with a more complex base distribution is computationally more demanding, and its effectiveness is apparently highly dependent on how close the more complex base distribution matches with the target distribution. The works in [Jaini et al., 2020, Liang et al., 2022] show that a heavy-tailed target distribution cannot be modeled with Real NVPs, unless the base distribution is also changed to a heavy tailed distribution. In general, training with a heavy-tailed base distribution is more challenging due to the increase in variance of the gradient estimates. We show in our experiments, that our proposed modifications enable stable training with a student-t distribution, leading to considerably better estimates of the marginal likelihood.

Another line of work suggests the use of path gradients [Roeder et al., 2017, Vaitl et al., 2022] which removes the score term from the gradient estimation of the Kullback-Leibler (KL)-divergence, and can lead to considerably lower variance of the gradient estimates. Our experiments confirm the usefulness of path gradients

¹Preliminary results of our work were presented in [Andrade, 2023].

also for high-dimensional posterior approximation. We note that in order to stabilize training, control variates, as proposed in [Ranganath et al., 2014], could in principle also be applied to NFs. However, in practice, due to the high number of parameters of NFs, such control variates are not computationally feasible.

The remainder of this article is structured as follows. In Section 2, we provide backgrounds on variational inference and Real NVPs. In Section 3, we describe the problem of exponentially large sample values, followed by Section 4, where we describe our proposed modifications. Moreover, in Section 5, we describe several other possible modifications of Real NVPs. In Section 6, we describe all models (target distributions) and methods that are used for marginal likelihood estimation in our experiments. In Section 7, we report the main results for five different models with 1000 or more dimensions, followed by Section 8, where we analyze the impact of different modifications on training and marginal likelihood estimation, and also compare to Hamiltonian Monte Carlo (HMC). Finally, in Section 9, we summarize our results, and provide recommendations for the architecture and training of NFs with VI. The code for reproducing all experiments is available here <https://github.com/andrade-stats/normalizing-flows>.

2. BACKGROUND ON NORMALIZING FLOWS AND REAL NVP

Variational inference with the reverse Kullback-Leibler (KL) divergence minimizes

$$(1) \quad \text{KL}(q_\eta || p_*) = \mathbb{E}_{q_\eta} \left[\log \left(\frac{q_\eta(\boldsymbol{\theta})}{p_*(\boldsymbol{\theta})} \right) \right],$$

where q_η denotes the variational approximation parameterized by the vector $\boldsymbol{\eta}$, and p_* denotes the target density given by

$$p_*(\boldsymbol{\theta}) := \frac{p(\boldsymbol{\theta}, D)}{p(D)},$$

where $p(\boldsymbol{\theta}, D)$ is the density of the joint distribution of model parameters $\boldsymbol{\theta} \in \mathbb{R}^d$ and data D , and $p(D)$ is the marginal likelihood. We therefore have

$$\text{KL}(q_\eta || p_*) = \mathbb{E}_{q_\eta} \left[\log \left(\frac{q_\eta(\boldsymbol{\theta})}{p(\boldsymbol{\theta}, D)} \right) \right] + \log p(D).$$

Normalizing flows approximate the posterior as follows:

$$\begin{aligned} \mathbf{z} &\sim q_0, \\ f_\eta(\mathbf{z}) &\sim q_\eta, \end{aligned}$$

i.e. we first sample \mathbf{z} from a base distribution q_0 , and then use $f_\eta(\mathbf{z})$ as a sample from the approximate posterior q_η . Assuming that $f : \mathbb{R}^d \rightarrow \mathbb{R}^d$ is a smooth bijective function, the density of the variational approximation is given by

$$q_\eta(f_\eta(\mathbf{z})) = q_0(\mathbf{z}) |\det(J_f(\mathbf{z}))|^{-1},$$

where $J_f(\mathbf{z}) \in \mathbb{R}^{d \times d}$ is the Jacobian (matrix with all partial derivatives) of f_η evaluated at point \mathbf{z} .

Using the law of the unconscious statistician, we get

$$\mathbb{E}_{q_\eta} \left[\log \left(\frac{q_\eta(\boldsymbol{\theta})}{p(\boldsymbol{\theta}, D)} \right) \right] = \mathbb{E}_{q_0} \left[\log \left(\frac{q_\eta(f_\eta(\mathbf{z}))}{p(f_\eta(\mathbf{z}), D)} \right) \right]$$

which is called the negative ELBO (evidence lower bound) [Blei et al., 2017, Papamakarios et al., 2021].

Finally, for minimizing $\text{KL}(q_\eta||p_*)$ with respect to the variational parameters $\boldsymbol{\eta}$, we need to evaluate the gradient

$$\begin{aligned} \frac{\partial}{\partial \boldsymbol{\eta}} \text{KL}(q_\eta||p_*) &= \frac{\partial}{\partial \boldsymbol{\eta}} \mathbb{E}_{q_\eta} \left[\log \left(\frac{q_\eta(\boldsymbol{\theta})}{p(\boldsymbol{\theta}, D)} \right) \right] \\ &= \mathbb{E}_{q_0} \left[\frac{\partial}{\partial \boldsymbol{\eta}} \log \left(\frac{q_\eta(f_\eta(\mathbf{z}))}{p(f_\eta(\mathbf{z}), D)} \right) \right]. \end{aligned}$$

Using samples $\mathbf{z}_k \sim q_0$ for $k = 1, \dots, b$, we can approximate the gradient using

$$(2) \quad \frac{\partial}{\partial \boldsymbol{\eta}} \text{KL}(q_\eta||p_*) \approx \frac{1}{b} \sum_{k=1}^b \left[\frac{\partial}{\partial \boldsymbol{\eta}} \log \left(\frac{q_\eta(f_\eta(\mathbf{z}_k))}{p(f_\eta(\mathbf{z}_k), D)} \right) \right].$$

Alternatively, as originally proposed in [Roeder et al., 2017], the following gradient estimate can have lower variance

$$(3) \quad \frac{1}{b} \sum_{k=1}^b \left[\frac{\partial}{\partial \boldsymbol{\eta}} \log \left(\frac{q_\eta(f_\eta(\mathbf{z}_j))}{p(f_\eta(\mathbf{z}_j), D)} \right) - \frac{\partial}{\partial \boldsymbol{\eta}} \log q_\eta(\boldsymbol{\theta}) \Big|_{\boldsymbol{\theta}=f_\eta(\mathbf{z}_j)} \right],$$

This gradient estimator removes the score term from Equation (2), and is also referred to as path gradients [Vaitl et al., 2022]. The motivation and derivation can be found in the Appendix.

2.1. Real NVP. For training we require that $f_\eta(\mathbf{z})$, $f_\eta^{-1}(\boldsymbol{\theta})$, and $\det(J_f(\mathbf{z}))$ can be evaluated efficiently.² Real NVP (real-valued non-volume preserving) is an architecture framework for f that has these required properties [Dinh et al., 2016].

Let S_0 and S_1 be a partition of the index set $\{1, 2, 3, \dots, d\}$, whereas $|S_0| = |S_1| = \frac{d}{2}$.³ Define

$$(4) \quad f := f_r \circ f_{r-1} \dots \circ f_1,$$

where the functions $f_i : \mathbb{R}^d \rightarrow \mathbb{R}^d$, for $1, 2, \dots, r$ are defined as follows. Let $\mathbf{z}^{(i+1)} := f_i(\mathbf{z}^{(i)})$, and define⁴

$$(5) \quad \begin{aligned} \mathbf{z}_A^{(i+1)} &:= \mathbf{z}_A^{(i)}, \\ \mathbf{z}_B^{(i+1)} &:= \mathbf{z}_B^{(i)} \odot \exp(s_i(\mathbf{z}_A^{(i)})) + t_i(\mathbf{z}_A^{(i)}), \end{aligned}$$

where

$$(6) \quad \begin{aligned} A &:= S_{(i+1) \bmod 2}, \quad \text{and} \\ B &:= S_{i \bmod 2}, \end{aligned}$$

and $s_i : \mathbb{R}^{d/2} \rightarrow \mathbb{R}^{d/2}$ and $t_i : \mathbb{R}^{d/2} \rightarrow \mathbb{R}^{d/2}$ are arbitrary functions that are modeled with a neural network. Note that the exponential \exp is taken component-wise, and \odot denotes the Hadamard product. The vector $\boldsymbol{\eta}$ contains all neural network weights and bias terms. Note that $\mathbf{z}^{(1)}$ is sampled from the base distribution q_0 , which is

²Note that when using path gradients we need to evaluate the inverse $f_\eta^{-1}(\boldsymbol{\theta})$.

³For ease of representation here, we assume that d is even. The requirement that S_0 and S_1 are of the same size is not essential. In our implementation, we assign all even indices to S_0 and all odd indices to S_1 .

⁴The notation \mathbf{z}_A denotes the set $\{z_j | j \in A\}$.

often assumed to be a normal distribution. The Equations (5) are often referred to as an affine coupling layer [Dinh et al., 2016, Lee et al., 2021, Ishikawa et al., 2023].

Note that our definition of Real NVP as given in Equations (4), (5) and (6), is the one often used in practice [Dinh et al., 2016, Huang et al., 2020, Koehler et al., 2021]. Despite its restrictive form, i.e. no permutation between affine coupling layers, and only alternation of the sets A and B , as described in Equation (6), Koehler et al. [2021] proved that $f\#q_0$ is a universal approximator to any target distribution on a compact set $U \subseteq \mathbb{R}^d$.⁵

Though, in theory, $r \geq 3$ is sufficient for accurate approximation, in practice, often a much larger number of coupling layers r is required [Koehler et al., 2021].

3. EXPONENTIALLY LARGE SAMPLE VALUES

For any dimension j , let us denote by u the maximum scaling value of the Real NVP, i.e.

$$u := \max_{i \in \{1, \dots, r\}} \left(\exp(s_i(\mathbf{z}_A^{(i)})) \right)_j.$$

Let us denote by m the maximum value that is sampled from q_0 or output by any t_i , i.e.

$$m := \max_{i \in \{1, \dots, r\}} \{z_j^{(1)}, (t_i(\mathbf{z}_A^{(i)}))_j\}.$$

Then we have that

$$z_j^{(r+1)} \leq m \sum_{i=0}^r u^i.$$

In other words, the maximum value that $z_j^{(r+1)}$ can attain is of order $O(mu^r)$. That means deep Real NVP, with r being large, are prone to produce samples that are large in magnitude.

In Figures 10 (a) and 9 (a), for $r \in \{4, 32, 64\}$, we show the (absolute) maximum value of $z_j^{(r+1)}$ for each iteration during training. We observe that sometimes very large values are sampled, leading to an unstable estimate of the ELBO estimate that can cause high variance of the gradient estimates in Equations (2) and (3).

4. STABILIZING REAL-NVP

The analysis from the previous section suggests two strategies for mitigating large sample values:

- Placing an upper bound on the scaling factors $\exp(s_i(\mathbf{z}_A^{(i)}))$.
- Performing a log-transformation of the samples.

⁵The notation $f\#q_0$ denotes the push-forward of the probability measure q_0 by function f . For universal approximation in distribution, $r \geq 3$ and weak regularity conditions on the target distribution are necessary.

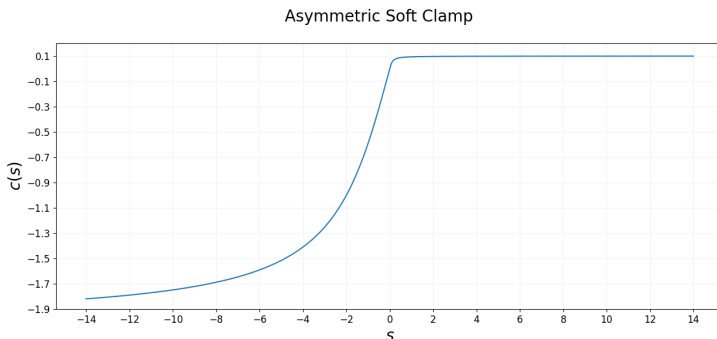


FIGURE 1. Shows the asymmetric soft clamp function $c(s)$ from Equation (7) with $\alpha_{neg} = 2$ and $\alpha_{pos} = 0.1$.

Upper and lower bounds on the scaling factors. We propose to threshold high scaling factors to ensure that $s_i(\mathbf{z}_A^{(i)}) \leq \alpha_{pos}$, where the threshold α_{pos} is set to a fixed small value. In order to ensure the stable calculation of the inverse f^{-1} it is also necessary to ensure that $\exp(s_i(\mathbf{z}_A^{(i)}))$ from Equation (5) does not get too close to zero. We therefore place an additional threshold that enforces $s_i(\mathbf{z}_A^{(i)}) \geq -\alpha_{neg}$. Rather than hard thresholding, we found empirically that the following asymmetric soft clamping improved training

$$(7) \quad c(s) = \frac{2}{\pi} \begin{cases} \alpha_{pos} \arctan(s/\alpha_{pos}) & \text{if } s \geq 0, \\ \alpha_{neg} \arctan(s/\alpha_{neg}) & \text{if } s < 0. \end{cases}$$

with $\alpha_{neg} < \alpha_{pos}$. Note that $c(s)$ is differentiable everywhere. For our experiments we set $\alpha_{neg} = 2$ and $\alpha_{pos} = 0.1$.⁶ Note that this is a modification of the soft-clamping proposed in [Ardizzone et al., 2019], with the important difference that high-values of s are suppressed more forcefully. The resulting function is shown in Figure 1. With the proposed asymmetric soft clamping, Equation (5) changes to

$$(8) \quad \mathbf{z}_B^{(i+1)} := \mathbf{z}_B^{(i)} \odot \exp(c(s_i(\mathbf{z}_A^{(i)}))) + t_i(\mathbf{z}_A^{(i)}).$$

Log-transformation of the samples. Since the maximum value of a sample $z^{(r+1)}$ is of order $O(mu^r)$, it is natural to consider some type of log-transformation $g(z)$ at the final layer. That means instead of (4), we use

$$(9) \quad f := g \circ f_r \circ f_{r-1} \dots \circ f_1.$$

Note that the function g must be a differentiable bijective function. In particular, we propose the following log soft extension (LOFT) layer:

$$(10) \quad g(z) = \begin{cases} \tau + \log(z - \tau + 1) & \text{if } \theta \geq \tau, \\ -\tau - \log(-z - \tau + 1) & \text{if } \theta \leq -\tau, \\ z & \text{else.} \end{cases}$$

$$= \text{sign}(z) \left(\log(\max(|z| - \tau, 0) + 1) + \min(|z|, \tau) \right).$$

⁶Overall good performance in terms of ELBO, though manually tuning for each task might improve results further.

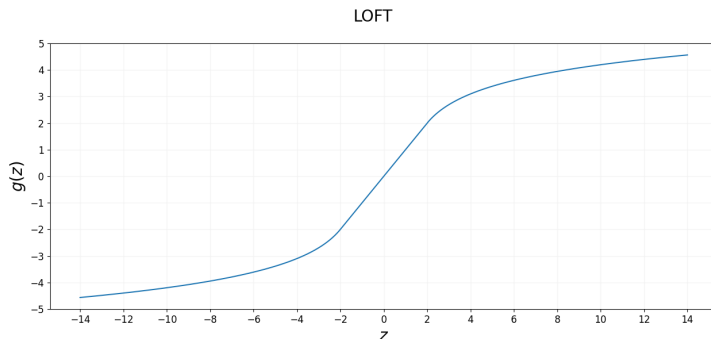


FIGURE 2. Shows the LOFT function $g(z)$ from Equation (10) with $\tau = 2$.

The function is shown in Figure 2: within the range $[-\tau, \tau]$ the layer performs an identity mapping, and outside the range, the absolute value of the function grows only logarithmically; τ is a fixed pre-specified parameter. For a vector \mathbf{z} we apply the LOFT function element-wise. Note that LOFT is a one-to-one function and

$$g^{-1}(z) = \text{sign}(z) \left(\exp(\max(|z| - \tau, 0)) - 1 + \min(|z|, \tau) \right),$$

$$\log\left(\frac{\partial}{\partial z} g(z)\right) = -\log(\max(|z| - \tau, 0) + 1).$$

Therefore, all necessary calculations can be expressed using only computationally efficient elementary operations (without if-clauses). For all of our experiments we set $\tau = 100$.

5. DETAILS ON ARCHITECTURE AND ALTERNATIVE CHOICES

Base Distribution and Clipping. While we propose to use the clipping from Equation (7), the works in [Ardizzone et al., 2019] propose to use symmetric clipping with the arctan function, whereas [Jaini et al., 2020] suggests to use the tanh function. For the base distribution q_0 there are two common choices:

- independent identical standard Gaussian distribution for each dimension, i.e. $\prod_{j=1}^d N(0, 1)$.
- independent non-identical student-t distribution $\prod_{j=1}^d \text{StudentT}(\nu_j)$, where $\text{StudentT}(\nu_j)$ denotes the standard student-t distribution with ν_j degrees of freedom.

An overview of some variations of Real NVP are given in Table 1.

Affine Transformation. All previous works transform the base distribution by an affine transformation

$$a(\mathbf{z}) = \boldsymbol{\sigma} \odot \mathbf{z} + \boldsymbol{\mu},$$

with trainable parameters $\boldsymbol{\sigma} \in \mathbb{R}_+^d$ and $\boldsymbol{\mu} \in \mathbb{R}^d$. The resulting normalizing flow therefore becomes

$$f := f_r \circ f_{r-1} \dots \circ f_1 \circ a.$$

TABLE 1. Overview of previously proposed variations of Real NVP.

Name	Base Distribution	Clipping	Reference
standard	Gaussian	none	[Dinh et al., 2016]
ATAF	StudentT	tanh	[Jaini et al., 2020, Liang et al., 2022]
SymClip	Gaussian	arctan	[Ardizzone et al., 2019]

When using the modifications from Section 4, we perform the affine transformation at the end, i.e.

$$f := a \circ g \circ f_r \circ f_{r-1} \dots \circ f_1,$$

which has the advantage of re-adjusting the scaling that might have been reduced by LOFT and the asymmetric soft clamping of s_i .

6. EXPERIMENTS

In this section, we first describe the different probabilistic models that we use for evaluation (Section 6.1), and then describe the training of the normalizing flows and other MCMC-based methods that are used for comparison (Section 6.2).

6.1. Models. For evaluation, we use four different target distributions, for which the log marginal likelihood is known (Basic Models), and a challenging Horseshoe Logistic Regression model with synthetic and real data.

6.1.1. Basic Models.

Funnel Distribution. The funnel distribution, as introduced in [Neal, 2003], is given by

$$p_*(\theta_1) = N(0, 9), \quad \forall j \in 2, \dots, d : p_*(\theta_j | \theta_1) = N(0, e^{\theta_1}).$$

The target distribution is $p_*(\boldsymbol{\theta})$ with $\boldsymbol{\theta} := (\theta_1, \theta_2, \dots, \theta_d) \in \mathbb{R}^d$.

Multivariate Student-T Distribution. The multivariate student-t distribution with mean $\mathbf{0}$, degrees of freedom ν , and scale matrix Σ is given by

$$p_*(\boldsymbol{\theta}) = \frac{\Gamma((\nu + d)/2)}{\Gamma(\nu/2)(\nu\pi)^{d/2}|\Sigma|^{1/2}} \left(1 + \frac{1}{\nu}\boldsymbol{\theta}^T \Sigma^{-1} \boldsymbol{\theta}\right)^{-(\nu+d)/2},$$

where we set the scale matrix to $\Sigma_{i,j} = 0.8$, for $i \neq j$, and $\Sigma_{i,i} = 1$.

Multivariate Gaussian Mixture.

$$p_*(\boldsymbol{\theta}) = \sum_{j=1}^k \frac{1}{k} N(\boldsymbol{\theta} | \boldsymbol{\mu}_j, I_d),$$

where I_d denotes the identity matrix in $\mathbb{R}^{d \times d}$. Here, we set $k = 3$, and $\boldsymbol{\mu}_1 = \frac{1}{\sqrt{d}}\mathbf{6}$, $\boldsymbol{\mu}_2 = -\frac{1}{\sqrt{d}}\mathbf{6}$, and $\boldsymbol{\mu}_3 = \mathbf{0}$ (i.e. in all dimensions constant values $\frac{1}{\sqrt{d}}6$, $-\frac{1}{\sqrt{d}}6$, and 0, respectively).

Conjugate Linear Regression. We consider the following Bayesian linear regression model

$$\begin{aligned}\sigma^2 &\sim \text{Inv-Gamma}(0.5, 0.5) \\ \boldsymbol{\beta} &\sim N(\mathbf{0}, \sigma^2 I_{d'-1}) \\ y_i &\stackrel{i.i.d.}{\sim} N(\mathbf{x}_i^T \boldsymbol{\beta}, \sigma^2) \quad \text{for } i \in \{1, \dots, n\}.\end{aligned}$$

The parameters are $\boldsymbol{\theta} := (\boldsymbol{\beta}, \sigma^2)$, and the target distribution is the posterior $p(\boldsymbol{\theta}|\mathbf{y}, X)$. Note that, different from before, $\boldsymbol{\theta} \in \mathbb{R}^{d'} \otimes \mathbb{R}_+$. For the normalizing flows, in order to ensure the positiveness for σ^2 , we use the softplus-transformation (as suggested, for example, in [Kucukelbir et al. \[2017\]](#)).

Due to the conjugacy of the priors, the log marginal likelihood has a closed form given by [Chipman et al. \[2001\]](#):

$$\log p(\mathbf{y}|X) = \frac{\Gamma((1+n)/2)}{\Gamma(1/2)\pi^{n/2}|\Sigma|^{1/2}} \left(1 + \mathbf{y}^T \Sigma^{-1} \mathbf{y}\right)^{-(1+n)/2},$$

where $\Sigma := (I_n - X(X^T X + I_d)^{-1} X^T)^{-1}$, and $X \in \mathbb{R}^{n \times d'}$ contains all explanatory variables.

6.1.2. Horseshoe Logistic Regression Model. We consider the following high-dimensional logistic regression model with the Horseshoe prior [\[Carvalho et al., 2010\]](#):

$$\begin{aligned}\tau &\sim C^+(0, 1) \\ \text{for } j \in \{1, \dots, d'\}: \\ \lambda_j &\sim C^+(0, 1) \\ \beta_j &\sim N(0, \tau^2 \lambda_j^2) \\ \mu &\sim C^+(0, 10) \\ y_i &\stackrel{i.i.d.}{\sim} \text{Bernoulli}(\sigma(\mathbf{x}_i^T \boldsymbol{\beta} + \mu)), \text{ for } i \in \{1, \dots, n\},\end{aligned}$$

where $C^+(0, s)$ is the half-Cauchy distribution with scale s , and σ is the sigmoid function. Note that here the total number of parameters d is $2d' + 2$. Again, to ensure the positiveness for τ , $\boldsymbol{\lambda}$, and μ , we use the softplus-transformation.

6.2. Description of Variational Inference and MCMC Methods. We compare our proposed modifications of Real NVP (*proposed*) to three other variations, namely *standard*, *ATAF* and *SymClip*, as described in [Table 1](#). Furthermore, we also compare to mean field Gaussian variational inference. We did not compare to other normalizing flows like residual flows or continuous flows [\[Papamakarios et al., 2021\]](#), since, in preliminary experiments, they produced inferior results, or do not allow for importance sampling to estimate the marginal likelihood.

For estimating the marginal likelihood, we also compare to a sequential monte carlo (SMC) sampler. SMC is an extension of annealed importance sampling [\[Neal, 2001\]](#), but with improved performance for estimating the normalization constant [\[Arbel et al., 2021\]](#). Indeed, removing the resampling step in SMC corresponds to annealed importance sampling [\[Dai et al., 2022\]](#).

For all variational inference (VI) methods (normalizing flows and mean field Gaussian), we used Adam [\[Kingma and Ba, 2015\]](#) with a mini-batch of size 256 and path gradients (i.e. $b = 256$, from [Equation \(3\)](#)) and a fixed learning rate of 10^{-4} . The number of training iterations is set to 60,000, except for the gene expression

data experiment where we used 400,000 iterations. For SMC, we used a geometric annealing scheme with 100,000 (intermediate) temperatures.

We also compared to an Hamiltonian Monte Carlo (HMC) sampler [Neal et al., 2011] with NUTS [Hoffman et al., 2014] in terms of Wasserstein distance to the true target distribution.

Estimation of ELBO and Marginal Likelihood. Like mean field VI, Real NVPs have the big advantage that sampling and estimation of the density $q_{\boldsymbol{\eta}}$ is fast. This allows us to use importance sampling (IS) to get an estimate of the marginal likelihood:

$$\begin{aligned} p(D) &= \mathbb{E}_{q_{\boldsymbol{\eta}}} \left[\frac{p(\boldsymbol{\theta}, D)}{q_{\boldsymbol{\eta}}(\boldsymbol{\theta})} \right] \\ &\approx \frac{1}{b_{eval}} \sum_{k=1}^{b_{eval}} \frac{p(\boldsymbol{\theta}_k, D)}{q_{\boldsymbol{\eta}}(\boldsymbol{\theta}_k)}, \end{aligned}$$

where $\boldsymbol{\theta}_k \sim q_{\boldsymbol{\eta}}$ for $k = 1, \dots, b_{eval}$. For the final evaluation of ELBO and the IS estimate, we use 20,000 samples (i.e. $b_{eval} = 20,000$), and repeat each evaluation 20 times to estimate the Monte Carlo error [Koehler et al., 2009].

7. RESULTS

We evaluated all methods on the models described in 6.1 for different number of dimensions d ranging from $d = 10$ to $d = 4002$. For $d < 300$, most methods performed similarly, therefore, we focus here on the results for $d \geq 1000$. The results for $d < 300$ can be found in the Appendix in Tables 7, 8, and 11. We show the results for four different variations of our proposed method using either a student-t or Gaussian base distribution, and using either LOFT or not.

7.1. Basic Models. Figures 3 and 4 show the results for the four basic models, where the true marginal likelihood is known. We see that all methods tend to underestimate the true marginal likelihood. In most cases, the results of the marginal likelihood estimates based on SMC and the mean field Gaussian approximation (for which average and standard deviation are shown on top of each graph) were considerably worse than the estimates based on normalizing flows. For example, for Funnel, the mean field Gaussian approximation and SMC had an error of more than 3, whereas the error for the normalizing flows was around 0.05 or less. Overall all normalizing flows performed similarly, except for the challenging multivariate student-t model (Figure 3, (b)), where the proposed method performed slightly better than other normalizing flows.

A higher ELBO tends to improve the estimate of the marginal likelihood. In deed, as we show in Figure 5, optimizing the ELBO is strongly correlated with better estimates of the marginal likelihood that are found via importance sampling.

We note that, in theory, training normalizing flows with the forward KL [Jerfel et al., 2021] should lead to better estimates of the marginal likelihood via importance sampling. However, in practice, we found that the ELBO, of the reverse KL, is much more stable in training and, as suggested by Figure 5, highly correlated to better estimates of the marginal likelihood.

7.2. Horseshoe Logistic Regression Model. Next, in Figure 6, we show the results for the Horseshoe logistic regression model on synthetic data with $d = 2002$. Finally, we also evaluate all methods on a gene expression data set with 2000 genes from 62 tissue samples either belonging to tumor or normal colon tissue [Alon

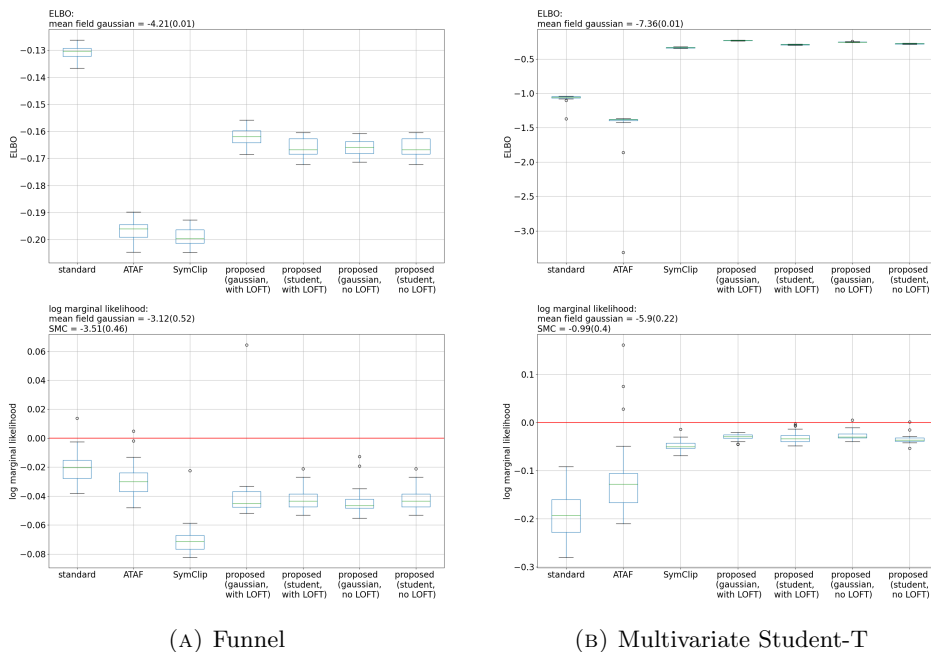


FIGURE 3. Shows the ELBO and the log marginal likelihood estimate using importance sampling ($d = 1000$). Red line shows true log marginal likelihood.

et al., 1999]; the estimated marginal likelihoods of the Horseshoe Logistic Regression model ($d = 4002$) are shown in Figure 7. As before, mean field Gaussian VI and SMC fail due to the high dimensionality. For lower dimensions, as shown in the Appendix in Table 11, both methods perform better. Among all normalizing flows the proposed method with a student-t as base distribution and LOFT, performs best. Compared to ATAF, for the synthetic data, the proposed method improves ELBO by around 30% and for the colon tissue data by around 20%, resulting in considerably higher estimates of the marginal likelihood.

8. ANALYSIS

Convergence and Large Sample Values. First, we take a closer look at the convergence behavior of the proposed method for the Horseshoe logistic regression model. Figure 8 confirms that the proposed method achieves faster convergence to a lower optimum of the loss (= negative ELBO) than other normalizing flow variations. Next, in Figures 9 and 10 we empirically confirm the observation from Section 3 that normalizing flows based on coupling layers tend to produce larger values with increasing depth. However, comparing the left (a) and right-hand side (b) of the Figures 9 and 10 we find that the proposed method successfully restrains large sample values at the last layer.

Important Details of Training Normalizing Flows. For the training of all normalizing flows, we use double precision (opposite to training of ordinary neural networks, where single precision is often considered sufficient). Furthermore, for training of

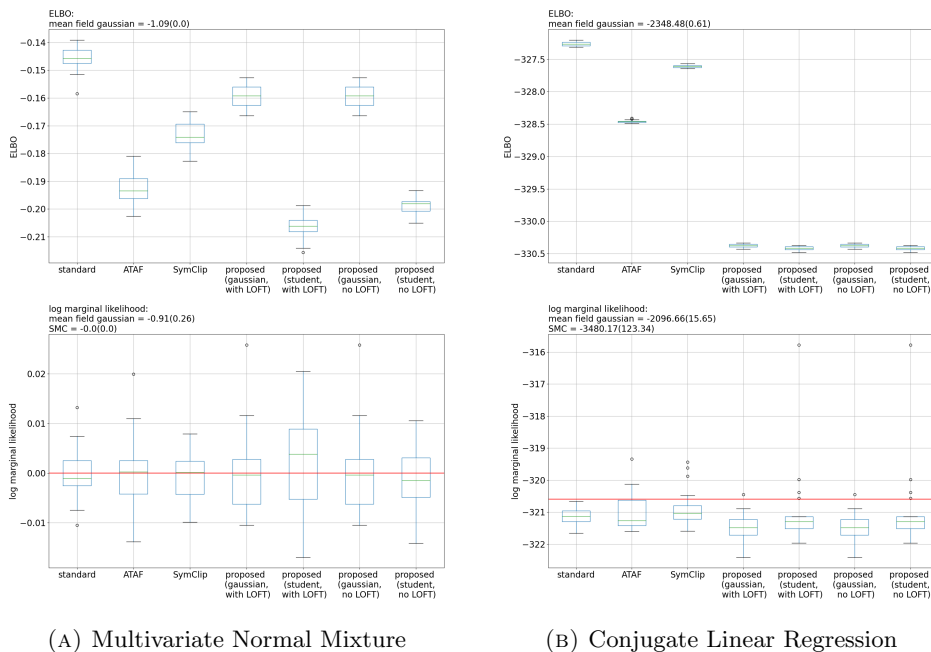


FIGURE 4. Shows the ELBO and the log marginal likelihood estimate using importance sampling ($d = 1000$, for the Conjugate Linear Regression model $d = 1001$). Red line shows true log marginal likelihood.

all normalizing flows we used path gradients (as proposed in [Roeder et al., 2017, Vaitl et al., 2022]), and do not employ annealing (opposite to the suggestion in [Rezende and Mohamed, 2015]). Our analysis in the appendix shows that these choices are crucial for stable training (see Tables 5 and 4).⁷

The works in [Dhaka et al., 2020] show that detecting convergence can be tricky even for variational inference with a Gaussian approximation family. Indeed, we found that training deep normalizing flows with the ELBO is similar to the mini-batch training of ordinary deep learning: detection of convergence is difficult since after a period of increase, the loss (negative ELBO) sometimes can drop again. As a consequence, given a fixed budget of M iterations, we compared: (1) taking the model after M iterations, and (2) taking the model with the lowest loss during the iterations $M/2$ and M iterations. Note that at each iteration the loss is evaluate using only 256 samples, whereas for the final evaluation the ELBO is estimated with 20,000 samples. The results in the Appendix (in Table 6) show that the ELBO of the standard Real NVP can be considerably improved by taking the model with the lowest loss, while for the proposed method the differences are negligible. Note that in favor for the standard model, we used for all of our experiments the lowest loss model.

⁷Moreover we do not use gradient clipping and l2-regularization as these had only deteriorate effects.

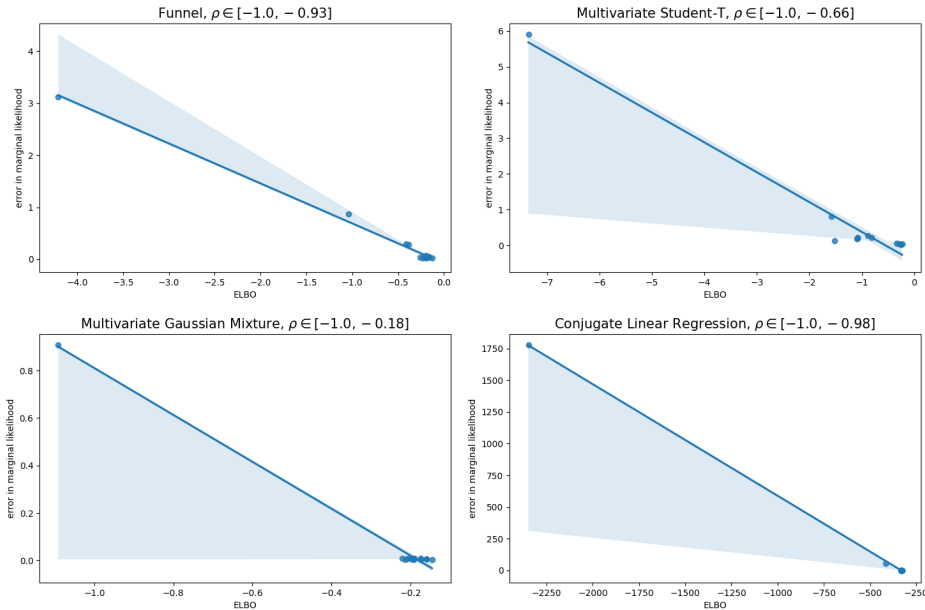


FIGURE 5. Plot of ELBO vs error in marginal likelihood of 13 different variational inference methods/models for each model; also shows 95% confidence level of pearson correlation ρ estimated with bootstrapping.

Importance of Depth of Normalizing Flows. We also evaluated the influence of the number of coupling layers r , i.e. the depth of the normalizing flow. We compared the ELBO and log marginal likelihoods results for $r = 64$ and $r = 16$, and found that for the proposed method an increase of r consistently improves ELBO and the log marginal likelihood estimate (see Appendix, Figure 11 for the horseshoe model, and 9, 7, 10, 8 for all basic models).

Comparison to HMC sampler. In the Appendix (in Table 3), we also compare the samples from the normalizing flows to the ground truth, and evaluate in terms of (sliced) Wasserstein distance $WD(q_\eta, p_*)$. We find that the quality of the samples of the normalizing flows are comparable to the sample of a long run HMC.⁸

Details on Runtime. A rough estimate of runtimes for all methods are shown in Table 2. We measured the runtime using NVIDIA RTX 6000 Ada with 48GB memory, on a Linux server with 32 cores. For all variational inference methods we used PyTorch [Paszke et al., 2017] and the normflows package [Stimper et al., 2023]. All implementations, except the HMC from Numpyro [Phan et al., 2019], were using the GPU, as such the runtime for HMC cannot be fairly compared to the other results. All variations of normalizing flows had about the same runtime. Note that sampling for normalizing flows is negligible (1~2 minutes) compared to training. Therefore, for repeated sampling, normalizing flows are computationally more efficient than SMC and HMC.

⁸Note that for the Multivariate Student-T model the estimation error of the Wasserstein distance is considerable, making it difficult to state a clear winner.

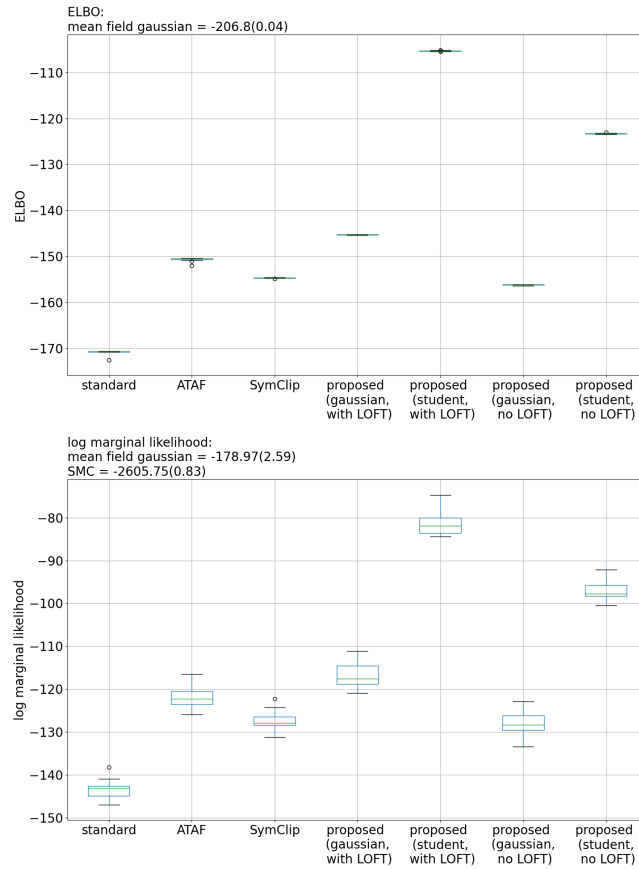


FIGURE 6. Shows the ELBO and the log marginal likelihood estimate using importance sampling for the Horseshoe logistic regression models on synthetic data with $d = 2002$.

TABLE 2. Approximate runtimes (wall-clock) for training/sampling of all methods (Horseshoe Logistic Regression model with $d = 2002$, 20 repetitions).

Method	Runtime in Minutes
mean field gaussian	10
proposed (student, with LOFT)	360
SMC	1510
HMC	33640

9. CONCLUSIONS AND RECOMMENDATIONS

Our experiments showed that for high dimensional posteriors (more than 1000 dimensions), normalizing flows based on coupling layers provide better estimates to the marginal likelihood than established methods like SMC. For the training

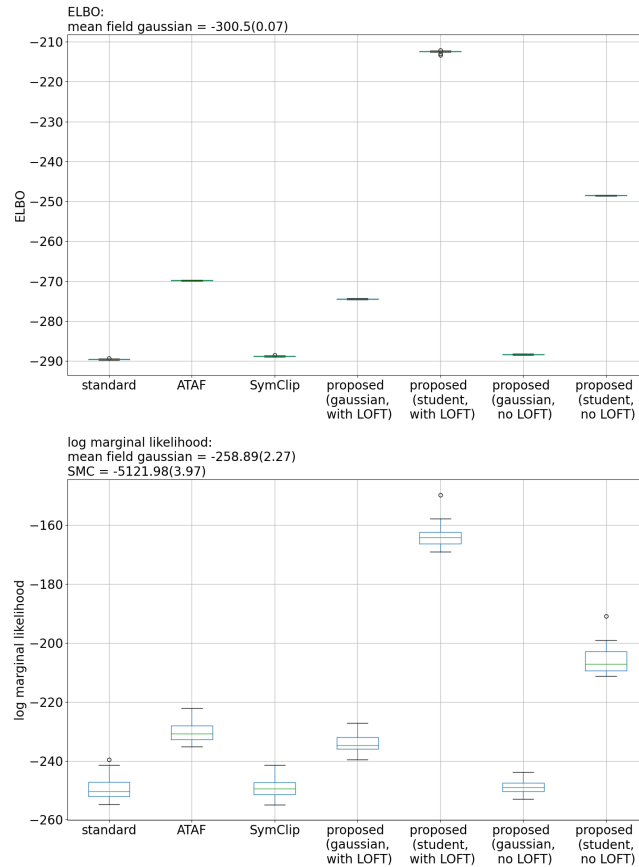


FIGURE 7. Shows the ELBO and the log marginal likelihood estimate using importance sampling for the Horseshoe logistic regression models on colon data with $d = 4002$.

objective of all normalizing flows, we used the reverse KL-divergence (ELBO), and verified that better estimates of the ELBO lead to better estimates of the marginal likelihood.

Furthermore, we found, theoretically and empirically, that normalizing flows based on coupling layers tend to produce samples with high absolute values, whereas the problem becomes more pronounced with increasing depth (=number of coupling layers). As a remedy, we proposed a soft clipping of the conditional factors s_i and a new log transformation layer named LOFT. Notably, these modification still preserve the bijectiveness of the flow and allow for computationally efficient calculation of all necessary derivatives. In particular for high dimensional posteriors with heavy tails we found that our proposed modifications (soft clipping + LOFT) lead to considerably improved estimates of the ELBO and the marginal likelihood.

Finally, we conducted extensive experiments with different modifications in architecture and training, where we found that the following choices lead to good estimates of ELBO/marginal likelihood:

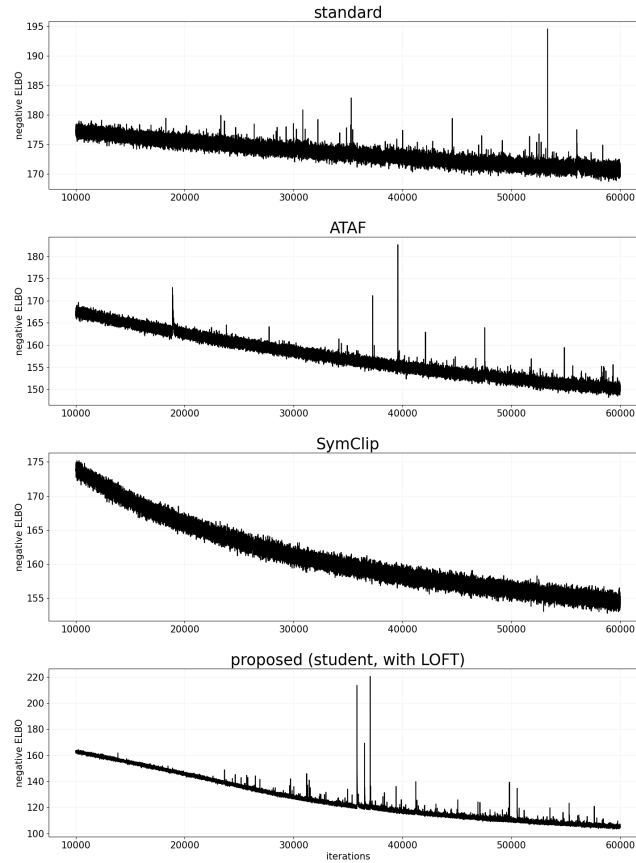


FIGURE 8. Shows the progress of the loss (= negative ELBO) over the training iterations for the Horseshoe logistic regression model with $d = 2002$.

- A student-t distribution as base distribution with trainable degree's of freedom for each dimension [Liang et al., 2022].
- A depth of 64 coupling layers (or possibly higher).⁹
- Gradient estimate without score term [Roeder et al., 2017, Vaitl et al., 2022].
- No annealing of training objective (opposite to suggestion in [Rezende and Mohamed, 2015]).
- Tracking and choosing the model with the smallest loss during training rather than the last model.

Though our focus was on the estimation of the marginal likelihood, our evaluation in terms of Wasserstein distance hints that normalizing flows with the above modifications provide samples with similar quality as HMC. Therefore, combining

⁹For our experiments, we used 64 coupling layers, and more coupling layers are likely to achieve an even higher ELBO. However, the high memory requirements during back-propagation place an upper bound on the number of coupling layers that can be used in practice.

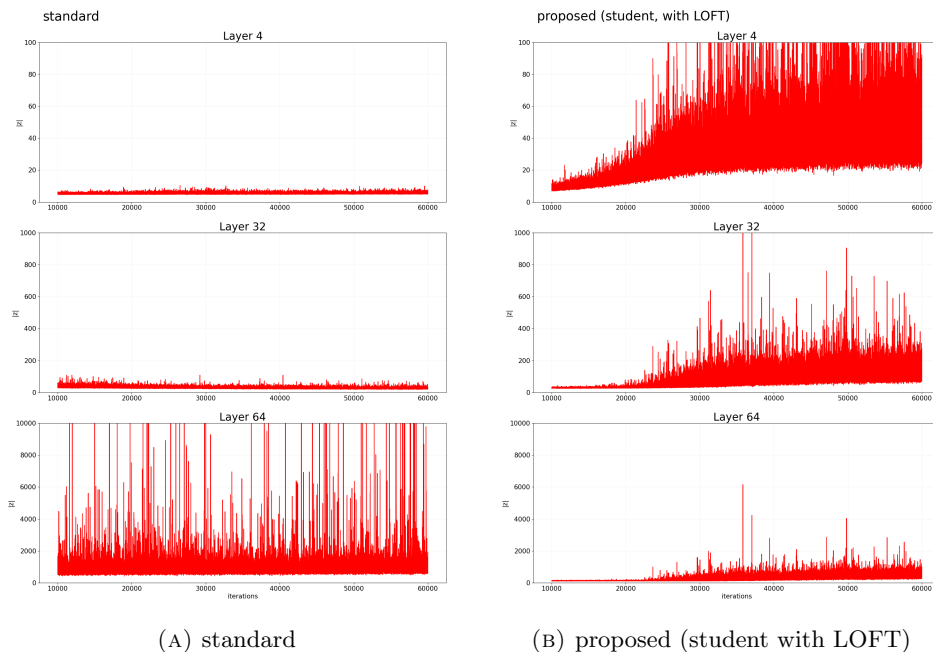


FIGURE 9. Shows the maximum value of a mini-batch sample after the 4-th, 32-th, and 64-th layer for the Horseshoe logistic regression model with $d = 2002$ when using (a) the standard normalizing flow, and (b) the proposed method.

the above normalizing flows with MCMC as, for example discussed in [Brofos et al., 2022, Winter et al., 2023], is a promising direction for future work.

FUNDING

This work was supported by JSPS KAKENHI Grant Number 22K11934.

APPENDIX

Details of Neural Network. For all normalizing flows, we used for each function s_i and t_i of Equation (5), a multi-layer perceptron with one hidden layer of size 100, and ReLU as activation function. All network parameters were initialized with 0, which means that, before training, output samples equal the distribution of the base distribution.

Details of Synthetic Data. For the synthetic data, we generated 20 datasets with dimensions $d \in \{10, 100, 1000\}$ and $n = 100$. The regression data was generated using the linear regression model described in Section 7.2, Example 1 of [Tibshirani, 1996]. The logistic regression data was generated as follows:

$$y_i \stackrel{i.i.d.}{\sim} \text{Bernoulli}(\sigma(\mathbf{x}_i^T \boldsymbol{\beta}_0 + \mu_0)), \text{ for } i \in \{1, \dots, n\},$$

with $\boldsymbol{\beta}_0 \in \mathbb{R}^d$, where the first, second, and fifth dimension of $\boldsymbol{\beta}_0$ are set to 3, 1.5, and 2, respectively; $\mu_0 := 1$, and \mathbf{x} are generated from a multivariate normal distribution with mean $\mathbf{0}$ and covariance matrix C , where $C_{ij} := 0.1^{|i-j|}$.

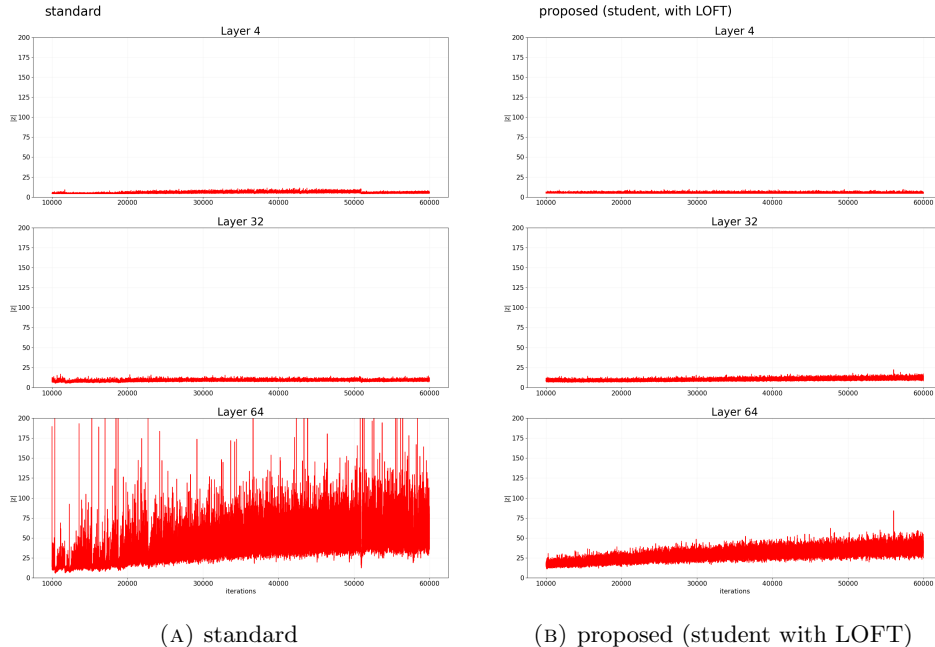


FIGURE 10. Shows the maximum value of a mini-batch sample after the 4-th, 32-th, and 64-th layer for the Funnel model with $d = 1000$ when using (a) the standard normalizing flow, and (b) the proposed method.

Details of SMC sampler. For comparison, we use a sequential monte carlo (SMC) sampler that is an extension of annealed importance sampling [Neal, 2001], but with improved performance for estimating the normalization constant [Arbel et al., 2021]. Indeed, removing the resampling step in SMC corresponds to annealed importance sampling [Dai et al., 2022].

For SMC, we used the GPU implementation of [Arbel et al., 2021] available at https://github.com/google-deepmind/annealed_flow_transport. As initial distribution q_0 , we use a standard normal distribution. To bridge between q_0 and the target distribution p_* , we use a geometric annealing scheme with 100,000 (intermediate) temperatures. The number of particles was set to 2000.¹⁰ At each time step (temperature), one iteration of HMC with NUTS is performed. Resampling at each time step is performed, if the effective sample size drops below $0.3N_p$. Comparison to HMC sampler. In Table 3, we also evaluate the samples from the normalizing flows to the ground truth, in terms of (sliced) Wasserstein distance $WD(q_\eta, p_*)$, and compare to samples of a long run HMC. For the HMC we used NUTS [Hoffman et al., 2014] with $200,000 \times 4$ chains; discarding first half of each chain as burn-in and thinning with interval 10.

¹⁰For Funnel, due to the long runtime, we used only 10,000 temperatures, and for $d = 1000$, we had to reduce the number of particles to 100.

Note that for the Conjugate Linear Regression Model (as described in 6.1.1) the true posteriors are available as

$$\begin{aligned}\log p(\sigma^2|\mathbf{y}, X) &= \text{Inv-Gamma}(\alpha_{\text{post}}, \beta_{\text{post}}), \\ \log p(\boldsymbol{\beta}|\mathbf{y}, X) &= \text{t}_\nu(\mu_{\text{post}}, \Sigma_{\text{post}}),\end{aligned}$$

where $\alpha_{\text{post}} = \frac{1+n}{2}$, $\beta_{\text{post}} = \frac{1}{2}(\|\mathbf{y}\|_2^2 + 1 - \mathbf{y}^T X U^{-1} X^T \mathbf{y})$, $U = X^T X + I$; t_ν denotes the multivariate student-t distribution with degrees of freedom $\nu = 1 + n$, mean $\mu_{\text{post}} = U^{-1} X^T \mathbf{y}$, and scale matrix $\Sigma_{\text{post}} = \frac{2\beta}{\nu} U^{-1}$.

Background on Path Gradients. Evaluating the gradient at some point $\boldsymbol{\eta}^*$, and using the chain-rule (from matrix calculus), we have

$$\left. \frac{\partial}{\partial \boldsymbol{\eta}} \log q_\boldsymbol{\eta}(f_\boldsymbol{\eta}(\mathbf{z})) \right|_{\boldsymbol{\eta}=\boldsymbol{\eta}^*} = \left(\frac{\partial}{\partial \boldsymbol{\theta}} \log q_{\boldsymbol{\eta}^*}(\boldsymbol{\theta}) \right) \frac{\partial}{\partial \boldsymbol{\eta}} f_\boldsymbol{\eta}(\mathbf{z}) + \left. \frac{\partial}{\partial \boldsymbol{\eta}} \log q_\boldsymbol{\eta}(\boldsymbol{\theta}) \right|_{\boldsymbol{\theta}=f_{\boldsymbol{\eta}^*}(\mathbf{z})}$$

and

$$\begin{aligned}\left. \frac{\partial}{\partial \boldsymbol{\eta}} \log p(f_\boldsymbol{\eta}(\mathbf{z}), D) \right|_{\boldsymbol{\eta}=\boldsymbol{\eta}^*} &= \left. \frac{\partial}{\partial \boldsymbol{\eta}} \log p(f_\boldsymbol{\eta}(\mathbf{z})|D) \right|_{\boldsymbol{\eta}=\boldsymbol{\eta}^*} \\ &= \left(\frac{\partial}{\partial \boldsymbol{\theta}} \log p(\boldsymbol{\theta}|D) \right) \frac{\partial}{\partial \boldsymbol{\eta}} f_\boldsymbol{\eta}(\mathbf{z}).\end{aligned}$$

Putting this together, we get

$$\begin{aligned}\left. \frac{\partial}{\partial \boldsymbol{\eta}} \text{KL}(q_\boldsymbol{\eta}||p_*) \right|_{\boldsymbol{\eta}=\boldsymbol{\eta}^*} &= \mathbb{E}_{q_0} \left[\left. \frac{\partial}{\partial \boldsymbol{\eta}} \log \left(\frac{q_\boldsymbol{\eta}(f_\boldsymbol{\eta}(\mathbf{z}))}{p(f_\boldsymbol{\eta}(\mathbf{z}), D)} \right) \right|_{\boldsymbol{\eta}=\boldsymbol{\eta}^*} \right] \\ &= \mathbb{E}_{q_0} \left[\left(\frac{\partial}{\partial \boldsymbol{\theta}} \log q_{\boldsymbol{\eta}^*}(\boldsymbol{\theta}) \right) \frac{\partial}{\partial \boldsymbol{\eta}} f_\boldsymbol{\eta}(\mathbf{z}) + \left. \frac{\partial}{\partial \boldsymbol{\eta}} \log q_\boldsymbol{\eta}(\boldsymbol{\theta}) \right|_{\boldsymbol{\theta}=f_{\boldsymbol{\eta}^*}(\mathbf{z})} - \left(\frac{\partial}{\partial \boldsymbol{\theta}} \log p(\boldsymbol{\theta}|D) \right) \frac{\partial}{\partial \boldsymbol{\eta}} f_\boldsymbol{\eta}(\mathbf{z}) \right] \\ &= \mathbb{E}_{q_0} \left[\left(\frac{\partial}{\partial \boldsymbol{\theta}} \log q_{\boldsymbol{\eta}^*}(\boldsymbol{\theta}) - \frac{\partial}{\partial \boldsymbol{\theta}} \log p(\boldsymbol{\theta}|D) \right) \frac{\partial}{\partial \boldsymbol{\eta}} f_\boldsymbol{\eta}(\mathbf{z}) + \left. \frac{\partial}{\partial \boldsymbol{\eta}} \log q_\boldsymbol{\eta}(\boldsymbol{\theta}) \right|_{\boldsymbol{\theta}=f_{\boldsymbol{\eta}^*}(\mathbf{z})} \right].\end{aligned}$$

Assuming that $q_{\boldsymbol{\eta}^*}(\boldsymbol{\theta}) \approx p(\boldsymbol{\theta}|D)$, we get

$$\left. \frac{\partial}{\partial \boldsymbol{\eta}} \text{KL}(q_\boldsymbol{\eta}||p_*) \right|_{\boldsymbol{\eta}=\boldsymbol{\eta}^*} \approx \mathbb{E}_{q_0} \left[\left. \frac{\partial}{\partial \boldsymbol{\eta}} \log q_\boldsymbol{\eta}(\boldsymbol{\theta}) \right|_{\boldsymbol{\theta}=f_{\boldsymbol{\eta}^*}(\mathbf{z})} \right],$$

whereas for samples $\mathbf{z}_k \sim q_0$, $k = 1, \dots, b$, the estimator is

$$\frac{1}{b} \sum_{k=1}^b \left[\left. \frac{\partial}{\partial \boldsymbol{\eta}} \log q_\boldsymbol{\eta}(\boldsymbol{\theta}) \right|_{\boldsymbol{\theta}=f_{\boldsymbol{\eta}^*}(\mathbf{z}_k)} \right].$$

Note that the variance of this estimator is not 0. Therefore, the works in [Roeder et al., 2017, Vaitl et al., 2022] propose to use instead the estimator

$$\frac{1}{b} \sum_{k=1}^b \left[\left. \frac{\partial}{\partial \boldsymbol{\eta}} \log \left(\frac{q_\boldsymbol{\eta}(f_\boldsymbol{\eta}(\mathbf{z}_k))}{p(f_\boldsymbol{\eta}(\mathbf{z}_k), D)} \right) - \left. \frac{\partial}{\partial \boldsymbol{\eta}} \log q_\boldsymbol{\eta}(\boldsymbol{\theta}) \right|_{\boldsymbol{\theta}=f_{\boldsymbol{\eta}^*}(\mathbf{z}_k)} \right],$$

which has variance 0 when $q_{\boldsymbol{\eta}^*}(\boldsymbol{\theta}) = p(\boldsymbol{\theta}|D)$.

TABLE 3. Evaluation of all methods in terms of Wasserstein distance to true distribution (standard deviation in brackets) for different dimensions d . For estimation the sliced Wasserstein distance is used; "nan" means that a numerically stable estimate could not be found; number of flows $r = 64$.

Funnel			
Method	$d = 10$	$d = 100$	$d = 1000$
mean field gaussian	7.96075 (0.5571)	9.16279 (1.95161)	8.81864 (0.76501)
standard	3.55096 (0.52902)	5.49619 (0.75929)	7.05587 (1.12632)
ATAF	6.16254 (1.27847)	5.43344 (1.35165)	7.08017 (0.71492)
SymClip	5.464 (0.79736)	6.39209 (0.76325)	7.35277 (0.88327)
proposed (gaussian, with LOFT)	5.26478 (1.5853)	7.9078 (5.04944)	7.17303 (0.69758)
proposed (student, with LOFT)	5.10961 (0.97158)	6.91015 (1.97344)	7.28766 (0.68416)
proposed (gaussian, no LOFT)	4.85281 (1.25448)	6.04271 (0.88001)	7.15134 (0.75477)
proposed (student, no LOFT)	5.30764 (1.43497)	6.48703 (1.31521)	7.50812 (1.26615)
HMC	3.80284 (1.06943)	3.07891 (1.14817)	6.23767 (2.1133)
Multivariate Student-T			
Method	$d = 10$	$d = 100$	$d = 1000$
mean field gaussian	978.22757 (2077.58198)	947.55754 (1981.72515)	339.85119 (319.99747)
standard	413.43534 (377.51084)	643.26898 (950.03763)	491.19396 (410.11727)
ATAF	813.73265 (1054.58138)	434.39064 (487.75902)	nan (nan)
SymClip	908.83123 (1339.8407)	813.47494 (1260.90776)	1675.82688 (3798.4308)
proposed (gaussian, with LOFT)	421.94993 (448.44594)	431.86027 (502.31684)	525.45636 (816.70971)
proposed (student, with LOFT)	1087.58516 (2393.59627)	465.30794 (626.16168)	581.85254 (789.12662)
proposed (gaussian, no LOFT)	424.74731 (537.22081)	368.34586 (307.89202)	1073.10593 (3099.12445)
proposed (student, no LOFT)	661.30146 (1076.37543)	235.95782 (153.88255)	630.76724 (1291.59487)
HMC	1319.2934 (1812.88423)	840.564 (622.86178)	788.89202 (1167.01651)
Multivariate Gaussian Mixture			
Method	$d = 10$	$d = 100$	$d = 1000$
mean field gaussian	1.00168 (0.00169)	0.16096 (0.00062)	0.02499 (0.00015)
standard	0.18057 (0.00635)	0.02511 (0.00172)	0.01405 (0.00015)
ATAF	0.12186 (0.00771)	0.04374 (0.00215)	0.02392 (0.00075)
SymClip	0.14645 (0.00652)	0.04968 (0.00214)	0.01622 (0.00047)
proposed (gaussian, with LOFT)	0.03911 (0.00337)	0.01673 (0.00054)	0.02191 (0.00065)
proposed (student, with LOFT)	0.20198 (0.00806)	0.01652 (0.00044)	0.01801 (0.00054)
proposed (gaussian, no LOFT)	0.03906 (0.00351)	0.01654 (0.00033)	0.02195 (0.00064)
proposed (student, no LOFT)	0.147 (0.00912)	0.05994 (0.00206)	0.01686 (0.00048)
HMC	0.0257 (0.00654)	0.01947 (0.00155)	0.01597 (0.00049)
Conjugate Linear Regression			
Method	$d = 11$	$d = 101$	$d = 1001$
mean field gaussian	0.15449 (0.00047)	0.31762 (0.00033)	0.12625 (0.00006)
standard	0.00787 (0.00045)	0.00693 (0.00024)	0.00972 (0.00008)
ATAF	0.00648 (0.00033)	0.00712 (0.00025)	0.00545 (0.00005)
SymClip	0.00603 (0.00027)	0.00679 (0.00015)	0.00591 (0.00005)
proposed (gaussian, with LOFT)	0.00723 (0.00042)	0.00658 (0.00024)	0.00635 (0.00004)
proposed (student, with LOFT)	0.00646 (0.00034)	0.00686 (0.0002)	0.00562 (0.00004)
proposed (gaussian, no LOFT)	0.00694 (0.00034)	0.00664 (0.00021)	0.00636 (0.00003)
proposed (student, no LOFT)	0.0066 (0.0004)	0.0069 (0.00022)	0.00561 (0.00004)
HMC	0.00521 (0.00036)	0.00595 (0.00025)	0.00259 (0.00002)

TABLE 4. Comparison of ELBO results with and without annealing for $d = 1000$ (for the Conjugate Linear Regression model $d = 1001$). "nan" means that a numerically stable estimate could not be found

Funnel		
Method	without annealing	with annealing
mean field gaussian	-4.20619 (0.00786)	-4.25079 (0.00797)
standard	-0.13076 (0.00262)	-0.71427 (0.00653)
ATAF	-0.19676 (0.00382)	-11.87143 (0.04698)
SymClip	-0.19903 (0.0034)	-0.26312 (0.00427)
proposed (gaussian, with LOFT)	-0.16222 (0.00316)	-0.15195 (0.00414)
proposed (student, with LOFT)	-0.16584 (0.0034)	-0.20455 (0.00309)
Multivariate Student-T		
Method	without annealing	with annealing
mean field gaussian	-7.35684 (0.00516)	-7.56552 (0.00736)
standard	-1.07369 (0.06991)	nan (nan)
ATAF	-1.51959 (0.44861)	nan (nan)
SymClip	-0.33732 (0.0055)	-0.36437 (0.00487)
proposed (gaussian, with LOFT)	-0.23245 (0.00392)	-0.39716 (0.00437)
proposed (student, with LOFT)	-0.29187 (0.00531)	-0.52886 (0.00652)
Multivariate Gaussian Mixture		
Method	without annealing	with annealing
mean field gaussian	-1.09121 (0.00081)	-1.091 (0.00089)
standard	-0.14578 (0.0044)	-1.16493 (0.00271)
ATAF	-0.19254 (0.00561)	-1.35144 (0.01046)
SymClip	-0.17354 (0.00437)	-0.1642 (0.00308)
proposed (gaussian, with LOFT)	-0.15943 (0.00418)	-0.1924 (0.00507)
proposed (student, with LOFT)	-0.20653 (0.00458)	-0.18603 (0.00446)
Conjugate Linear Regression		
Method	without annealing	with annealing
mean field gaussian	-2348.47948 (0.61318)	-2339.86726 (0.45202)
standard	-327.26313 (0.0318)	nan (nan)
ATAF	-328.46092 (0.0203)	nan (nan)
SymClip	-327.61051 (0.02208)	-27497.59608 (25.57452)
proposed (gaussian, with LOFT)	-330.37689 (0.02949)	-334.25809 (0.03358)
proposed (student, with LOFT)	-330.41806 (0.0309)	-333.41908 (0.04207)

TABLE 5. Comparison of ELBO results with and without score term for $d = 1000$ (for the Conjugate Linear Regression model $d = 1001$).

Funnel		
Method	without score term	with score term
mean field gaussian	-4.20619 (0.00786)	-4.21122 (0.00646)
standard	-0.13076 (0.00262)	-1.23624 (0.00825)
ATAF	-0.19676 (0.00382)	-1.34531 (0.00832)
SymClip	-0.19903 (0.0034)	-0.84768 (0.00697)
proposed (gaussian, with LOFT)	-0.16222 (0.00316)	-0.82072 (0.0075)
proposed (student, with LOFT)	-0.16584 (0.0034)	-0.93281 (0.00817)
Multivariate Student-T		
Method	without score term	with score term
mean field gaussian	-7.35684 (0.00516)	-7.63274 (0.00774)
standard	-1.07369 (0.06991)	-3.67112 (0.0079)
ATAF	-1.51959 (0.44861)	-3.71659 (0.01131)
SymClip	-0.33732 (0.0055)	-3.59259 (0.01113)
proposed (gaussian, with LOFT)	-0.23245 (0.00392)	-3.55175 (0.00922)
proposed (student, with LOFT)	-0.29187 (0.00531)	-3.59585 (0.00792)
Multivariate Gaussian Mixture		
Method	without score term	with score term
mean field gaussian	-1.09121 (0.00081)	-1.09444 (0.00111)
standard	-0.14578 (0.0044)	-1.22924 (0.00413)
ATAF	-0.19254 (0.00561)	-1.27836 (0.00491)
SymClip	-0.17354 (0.00437)	-1.20088 (0.00392)
proposed (gaussian, with LOFT)	-0.15943 (0.00418)	-1.20163 (0.00347)
proposed (student, with LOFT)	-0.20653 (0.00458)	-1.24067 (0.0039)
Conjugate Linear Regression		
Method	without score term	with score term
mean field gaussian	-2348.47948 (0.61318)	-2290.86055 (0.53819)
standard	-327.26313 (0.0318)	-336.70439 (0.04761)
ATAF	-328.46092 (0.0203)	-335.94146 (0.03875)
SymClip	-327.61051 (0.02208)	-335.4258 (0.03106)
proposed (gaussian, with LOFT)	-330.37689 (0.02949)	-336.43568 (0.03155)
proposed (student, with LOFT)	-330.41806 (0.0309)	-336.42227 (0.03385)

TABLE 6. Comparison of ELBO results using either the model with the lowest loss during training, or the last model for $d = 1000$ (for the Conjugate Linear Regression model $d = 1001$).

Funnel		
Method	lowest loss model	last model
mean field gaussian	-4.20619 (0.00786)	-4.20447 (0.00711)
standard	-0.13076 (0.00262)	-0.17381 (0.00354)
ATAF	-0.19676 (0.00382)	-0.2487 (0.00584)
SymClip	-0.19903 (0.0034)	-0.17057 (0.004)
proposed (gaussian, with LOFT)	-0.16222 (0.00316)	-0.17952 (0.00274)
proposed (student, with LOFT)	-0.16584 (0.0034)	-0.15643 (0.00314)
Multivariate Student-T		
Method	lowest loss model	last model
mean field gaussian	-7.35684 (0.00516)	-7.32763 (0.0068)
standard	-1.07369 (0.06991)	-1.40608 (0.03054)
ATAF	-1.51959 (0.44861)	-5.34154 (0.02333)
SymClip	-0.33732 (0.0055)	-0.29835 (0.00542)
proposed (gaussian, with LOFT)	-0.23245 (0.00392)	-0.25133 (0.00541)
proposed (student, with LOFT)	-0.29187 (0.00531)	-0.27859 (0.0046)
Multivariate Gaussian Mixture		
Method	lowest loss model	last model
mean field gaussian	-1.09121 (0.00081)	-1.09118 (0.00091)
standard	-0.14578 (0.0044)	-0.23477 (0.00475)
ATAF	-0.19254 (0.00561)	-0.18509 (0.00486)
SymClip	-0.17354 (0.00437)	-0.15595 (0.00344)
proposed (gaussian, with LOFT)	-0.15943 (0.00418)	-0.1871 (0.00403)
proposed (student, with LOFT)	-0.20653 (0.00458)	-0.19927 (0.00413)
Conjugate Linear Regression		
Method	lowest loss model	last model
mean field gaussian	-2348.47948 (0.61318)	-2347.61854 (0.47442)
standard	-327.26313 (0.0318)	-329.39336 (0.02498)
ATAF	-328.46092 (0.0203)	-332.94404 (0.03647)
SymClip	-327.61051 (0.02208)	-331.89927 (0.04517)
proposed (gaussian, with LOFT)	-330.37689 (0.02949)	-331.51712 (0.03626)
proposed (student, with LOFT)	-330.41806 (0.0309)	-331.7316 (0.03451)

TABLE 7. Evaluation of all methods in terms of ELBO (standard deviation in brackets) for $d \in \{10, 100, 1000\}$; number of flows $r = 64$.

Funnel			
Method	$d = 10$	$d = 100$	$d = 1000$
mean field gaussian	-1.86318 (0.00707)	-3.0504 (0.00729)	-4.20619 (0.00786)
standard	-0.01344 (0.00117)	-0.0566 (0.00193)	-0.13076 (0.00262)
ATAF	-0.05574 (0.00697)	-0.05184 (0.00165)	-0.19676 (0.00382)
SymClip	-0.02905 (0.00114)	-0.07004 (0.00131)	-0.19903 (0.0034)
proposed (gaussian, with LOFT)	-0.00896 (0.00066)	-0.04321 (0.00187)	-0.16222 (0.00316)
proposed (student, with LOFT)	-0.01244 (0.00072)	-0.0404 (0.00153)	-0.16584 (0.0034)
proposed (gaussian, no LOFT)	-0.01111 (0.00084)	-0.04291 (0.00156)	-0.16612 (0.0029)
proposed (student, no LOFT)	-0.01318 (0.00082)	-0.0402 (0.00154)	-0.16584 (0.0034)
Multivariate Student-T			
Method	$d = 10$	$d = 100$	$d = 1000$
mean field gaussian	-2.16601 (0.00651)	-4.5299 (0.00767)	-7.35684 (0.00516)
standard	-0.02437 (0.00138)	-0.08749 (0.00483)	-1.07369 (0.06991)
ATAF	-0.03101 (0.00173)	-0.10369 (0.0026)	-1.51959 (0.44861)
SymClip	-0.01674 (0.00075)	-0.05244 (0.00131)	-0.33732 (0.0055)
proposed (gaussian, with LOFT)	-0.01722 (0.00052)	-0.04715 (0.00146)	-0.23245 (0.00392)
proposed (student, with LOFT)	-0.01815 (0.00102)	-0.06186 (0.00189)	-0.29187 (0.00531)
proposed (gaussian, no LOFT)	-0.0164 (0.00061)	-0.05737 (0.00199)	-0.2555 (0.00421)
proposed (student, no LOFT)	-0.0158 (0.00077)	-0.05686 (0.00217)	-0.27904 (0.00403)
Multivariate Gaussian Mixture			
Method	$d = 10$	$d = 100$	$d = 1000$
mean field gaussian	-1.09054 (0.00072)	-1.09085 (0.00086)	-1.09121 (0.00081)
standard	-0.01622 (0.00128)	-0.04753 (0.00198)	-0.14578 (0.0044)
ATAF	-0.01508 (0.00118)	-0.08112 (0.00245)	-0.19254 (0.00561)
SymClip	-0.01116 (0.00095)	-0.05408 (0.0024)	-0.17354 (0.00437)
proposed (gaussian, with LOFT)	-0.00966 (0.00098)	-0.06171 (0.0025)	-0.15943 (0.00418)
proposed (student, with LOFT)	-0.01534 (0.00108)	-0.06713 (0.00258)	-0.20653 (0.00458)
proposed (gaussian, no LOFT)	-0.00966 (0.00098)	-0.06171 (0.0025)	-0.15943 (0.00418)
proposed (student, no LOFT)	-0.01138 (0.00105)	-0.07312 (0.00248)	-0.19908 (0.00292)
Conjugate Linear Regression			
Method	$d = 11$	$d = 101$	$d = 1001$
mean field gaussian	-275.82849 (0.0274)	-399.32425 (0.05422)	-2348.47948 (0.61318)
standard	-269.74157 (0.00046)	-347.86269 (0.00181)	-327.26313 (0.0318)
ATAF	-269.74116 (0.00032)	-347.86356 (0.0016)	-328.46092 (0.0203)
SymClip	-269.74059 (0.00035)	-347.87454 (0.00245)	-327.61051 (0.02208)
proposed (gaussian, with LOFT)	-269.74193 (0.0005)	-347.84601 (0.00193)	-330.37689 (0.02949)
proposed (student, with LOFT)	-269.74097 (0.00039)	-347.8542 (0.00208)	-330.41806 (0.0309)
proposed (gaussian, no LOFT)	-269.74193 (0.0005)	-347.84601 (0.00193)	-330.37689 (0.02949)
proposed (student, no LOFT)	-269.74097 (0.00039)	-347.8542 (0.00208)	-330.41806 (0.0309)

TABLE 8. Estimated log marginal likelihood (standard deviation in brackets) for $d \in \{10, 100, 1000\}$; number of flows $r = 64$.

Funnel			
Method	$d = 10$	$d = 100$	$d = 1000$
true value	0.0	0.0	0.0
mean field gaussian	-0.9051 (0.25602)	-1.93821 (0.67967)	-3.11768 (0.52003)
standard	-0.00068 (0.00282)	-0.00615 (0.00308)	-0.02001 (0.01194)
ATAF	-0.00992 (0.01665)	0.00199 (0.01963)	-0.02826 (0.01323)
SymClip	-0.00545 (0.0103)	-0.03279 (0.00632)	-0.06983 (0.01259)
proposed (gaussian, with LOFT)	-0.00184 (0.00381)	-0.01278 (0.0038)	-0.03778 (0.02408)
proposed (student, with LOFT)	-0.00267 (0.00598)	-0.01402 (0.00323)	-0.04245 (0.00766)
proposed (gaussian, no LOFT)	-0.00129 (0.00292)	-0.01385 (0.00356)	-0.04302 (0.01002)
proposed (student, no LOFT)	-0.00283 (0.00468)	-0.01393 (0.00334)	-0.04245 (0.00766)
SMC	-0.1429 (0.06911)	-1.76495 (0.36939)	-3.50737 (0.46121)
Multivariate Student-T			
Method	$d = 10$	$d = 100$	$d = 1000$
true value	0.0	0.0	0.0
mean field gaussian	-0.92496 (0.16171)	-2.87842 (0.3654)	-5.89942 (0.22141)
standard	-0.00642 (0.00224)	-0.01491 (0.00444)	-0.19315 (0.04714)
ATAF	-0.00416 (0.01041)	-0.0157 (0.00605)	-0.10957 (0.09367)
SymClip	-0.01059 (0.00149)	-0.00923 (0.03558)	-0.04795 (0.01257)
proposed (gaussian, with LOFT)	-0.01207 (0.00144)	-0.01696 (0.00277)	-0.03073 (0.00651)
proposed (student, with LOFT)	-0.01127 (0.00197)	-0.01844 (0.00362)	-0.0306 (0.01334)
proposed (gaussian, no LOFT)	-0.01031 (0.00111)	-0.01754 (0.00449)	-0.02604 (0.01032)
proposed (student, no LOFT)	-0.00979 (0.00207)	-0.01734 (0.00476)	-0.03379 (0.01077)
SMC	-0.01938 (0.01633)	-0.14798 (0.09068)	-0.98769 (0.39748)
Multivariate Gaussian Mixture			
Method	$d = 10$	$d = 100$	$d = 1000$
true value	0.0	0.0	0.0
mean field gaussian	-0.93939 (0.23324)	-0.89837 (0.29501)	-0.90655 (0.26212)
standard	0.00003 (0.0012)	-0.00063 (0.00182)	-0.00015 (0.00529)
ATAF	-0.00016 (0.00092)	0.00111 (0.00343)	0.00012 (0.007)
SymClip	0.00004 (0.00116)	-0.00179 (0.00194)	-0.00073 (0.00512)
proposed (gaussian, with LOFT)	-0.0 (0.00115)	-0.00083 (0.00262)	0.00007 (0.00818)
proposed (student, with LOFT)	-0.00032 (0.00093)	-0.00196 (0.00337)	0.00229 (0.01066)
proposed (gaussian, no LOFT)	-0.0 (0.00115)	-0.00083 (0.00262)	0.00007 (0.00818)
proposed (student, no LOFT)	-0.00012 (0.00113)	-0.00022 (0.00293)	-0.00135 (0.00625)
SMC	-0.00035 (0.00177)	-0.00019 (0.00257)	-0.00046 (0.0023)
Conjugate Linear Regression			
Method	$d = 11$	$d = 101$	$d = 1001$
true value	-269.73904	-347.81384	-320.59267
mean field gaussian	-271.18867 (0.48871)	-377.48859 (1.99237)	-2096.65892 (15.65285)
standard	-269.73934 (0.00054)	-347.81378 (0.00127)	-321.12109 (0.27435)
ATAF	-269.73912 (0.00026)	-347.81345 (0.00242)	-321.00036 (0.58395)
SymClip	-269.73882 (0.00038)	-347.81441 (0.00228)	-320.86489 (0.57739)
proposed (gaussian, with LOFT)	-269.73879 (0.00038)	-347.81429 (0.00213)	-321.45662 (0.43597)
proposed (student, with LOFT)	-269.73907 (0.00041)	-347.81414 (0.00249)	-320.99025 (1.28594)
proposed (gaussian, no LOFT)	-269.73879 (0.00038)	-347.81429 (0.00213)	-321.45662 (0.43597)
proposed (student, no LOFT)	-269.73907 (0.00041)	-347.81414 (0.00249)	-320.99025 (1.28594)
SMC	-281.18175 (3.00131)	-595.63322 (22.78467)	-3480.17078 (123.3412)

TABLE 9. Evaluation of all methods in terms of ELBO (standard deviation in brackets) for $d \in \{10, 100, 1000\}$; number of flows $r = 16$.

Funnel			
Method	$d = 10$	$d = 100$	$d = 1000$
mean field gaussian	-1.86318 (0.00707)	-3.0504 (0.00729)	-4.20619 (0.00786)
standard	-0.02689 (0.00183)	-0.04959 (0.00198)	-0.25683 (0.0073)
ATAF	-0.01924 (0.00171)	-0.05021 (0.0017)	-0.2305 (0.00641)
SymClip	-0.42434 (0.00289)	-0.84732 (0.00232)	-1.03967 (0.00336)
proposed (gaussian, with LOFT)	-0.02236 (0.00114)	-0.10715 (0.00125)	-0.38719 (0.00264)
proposed (student, with LOFT)	-0.02472 (0.00074)	-0.14684 (0.0019)	-0.41061 (0.00382)
proposed (gaussian, no LOFT)	-0.02236 (0.00114)	-0.10715 (0.00125)	-0.38719 (0.00264)
proposed (student, no LOFT)	-0.02472 (0.00074)	-0.14684 (0.0019)	-0.41061 (0.00382)
Multivariate Student-T			
Method	$d = 10$	$d = 100$	$d = 1000$
mean field gaussian	-2.16601 (0.00651)	-4.5299 (0.00767)	-7.35684 (0.00516)
standard	-0.03773 (0.00216)	-0.16146 (0.00566)	-1.08358 (0.00683)
ATAF	-0.03397 (0.00147)	-0.19026 (0.00388)	-1.09653 (0.00962)
SymClip	-0.2069 (0.00163)	-0.52876 (0.00305)	-1.58265 (0.00651)
proposed (gaussian, with LOFT)	-0.07184 (0.00096)	-0.23981 (0.00259)	-0.812 (0.00458)
proposed (student, with LOFT)	-0.06782 (0.00093)	-0.2354 (0.00199)	-0.89013 (0.0052)
proposed (gaussian, no LOFT)	-0.07184 (0.00096)	-0.23981 (0.00259)	-0.812 (0.00458)
proposed (student, no LOFT)	-0.06782 (0.00093)	-0.2354 (0.00199)	-0.89013 (0.0052)
Multivariate Gaussian Mixture			
Method	$d = 10$	$d = 100$	$d = 1000$
mean field gaussian	-1.09054 (0.00072)	-1.09085 (0.00086)	-1.09121 (0.00081)
standard	-0.03246 (0.00167)	-0.05054 (0.00246)	-0.22116 (0.00461)
ATAF	-0.01976 (0.00173)	-0.06112 (0.00237)	-0.19273 (0.00392)
SymClip	-0.02465 (0.00143)	-0.07069 (0.00255)	-0.17468 (0.00528)
proposed (gaussian, with LOFT)	-0.01937 (0.00119)	-0.08139 (0.00244)	-0.19073 (0.00416)
proposed (student, with LOFT)	-0.01625 (0.00132)	-0.06934 (0.00283)	-0.21368 (0.00352)
proposed (gaussian, no LOFT)	-0.01937 (0.00119)	-0.08139 (0.00244)	-0.19073 (0.00416)
proposed (student, no LOFT)	-0.01625 (0.00132)	-0.06934 (0.00283)	-0.21368 (0.00352)
Conjugate Linear Regression			
Method	$d = 11$	$d = 101$	$d = 1001$
mean field gaussian	-275.82849 (0.0274)	-399.32425 (0.05422)	-2348.47948 (0.61318)
standard	-269.7403 (0.00028)	-347.84904 (0.00169)	-332.96779 (0.04609)
ATAF	-269.74006 (0.00035)	-347.86773 (0.00228)	-331.99212 (0.03487)
SymClip	-269.74247 (0.00049)	-347.9524 (0.00331)	-416.32816 (0.09648)
proposed (gaussian, with LOFT)	-269.7403 (0.00037)	-347.85343 (0.00186)	-331.47248 (0.02527)
proposed (student, with LOFT)	-269.74073 (0.00047)	-347.84652 (0.00161)	-331.62923 (0.03325)
proposed (gaussian, no LOFT)	-269.7403 (0.00037)	-347.85343 (0.00186)	-331.47248 (0.02527)
proposed (student, no LOFT)	-269.74073 (0.00047)	-347.84652 (0.00161)	-331.62923 (0.03325)

TABLE 10. Estimated log marginal likelihood (standard deviation in brackets) for $d \in \{10, 100, 1000\}$; number of flows $r = 16$.

Funnel			
Method	$d = 10$	$d = 100$	$d = 1000$
true value	0.0	0.0	0.0
mean field gaussian	-0.9051 (0.25602)	-1.93821 (0.67967)	-3.11768 (0.52003)
standard	0.00018 (0.01105)	-0.00295 (0.00439)	-0.03178 (0.02555)
ATAF	-0.00471 (0.00219)	-0.00002 (0.00672)	-0.01926 (0.01717)
SymClip	-0.23247 (0.03862)	-0.66797 (0.05036)	-0.86603 (0.06121)
proposed (gaussian, with LOFT)	-0.01075 (0.00345)	-0.0732 (0.00722)	-0.2795 (0.01588)
proposed (student, with LOFT)	-0.00391 (0.02007)	-0.07329 (0.08636)	-0.29113 (0.02494)
proposed (gaussian, no LOFT)	-0.01075 (0.00345)	-0.0732 (0.00722)	-0.2795 (0.01588)
proposed (student, no LOFT)	-0.00391 (0.02007)	-0.07329 (0.08636)	-0.29113 (0.02494)
SMC	-0.1429 (0.06911)	-1.76495 (0.36939)	-3.50737 (0.46121)
Multivariate Student-T			
Method	$d = 10$	$d = 100$	$d = 1000$
true value	0.0	0.0	0.0
mean field gaussian	-0.92496 (0.16171)	-2.87842 (0.3654)	-5.89942 (0.22141)
standard	-0.01292 (0.00612)	-0.01293 (0.05005)	-0.21087 (0.06764)
ATAF	-0.01524 (0.00282)	-0.00086 (0.15296)	-0.17079 (0.07035)
SymClip	-0.11578 (0.02809)	-0.27219 (0.1134)	-0.80163 (0.14787)
proposed (gaussian, with LOFT)	-0.04565 (0.01678)	-0.13769 (0.021)	-0.22575 (0.04374)
proposed (student, with LOFT)	-0.03505 (0.02326)	-0.13828 (0.02616)	-0.25835 (0.08885)
proposed (gaussian, no LOFT)	-0.04565 (0.01678)	-0.13769 (0.021)	-0.22575 (0.04374)
proposed (student, no LOFT)	-0.03505 (0.02326)	-0.13828 (0.02616)	-0.25835 (0.08885)
SMC	-0.01938 (0.01633)	-0.14798 (0.09068)	-0.98769 (0.39748)
Multivariate Gaussian Mixture			
Method	$d = 10$	$d = 100$	$d = 1000$
true value	0.0	0.0	0.0
mean field gaussian	-0.93939 (0.23324)	-0.89837 (0.29501)	-0.90655 (0.26212)
standard	-0.00019 (0.00186)	-0.00066 (0.00174)	-0.00239 (0.01083)
ATAF	0.00012 (0.0013)	0.00009 (0.00291)	0.00243 (0.00582)
SymClip	0.00058 (0.00226)	-0.00059 (0.00267)	-0.00351 (0.00885)
proposed (gaussian, with LOFT)	-0.0001 (0.00133)	-0.00123 (0.00284)	0.00088 (0.01197)
proposed (student, with LOFT)	-0.00012 (0.0015)	0.00109 (0.00353)	-0.00217 (0.00491)
proposed (gaussian, no LOFT)	-0.0001 (0.00133)	-0.00123 (0.00284)	0.00088 (0.01197)
proposed (student, no LOFT)	-0.00012 (0.0015)	0.00109 (0.00353)	-0.00217 (0.00491)
SMC	-0.00035 (0.00177)	-0.00019 (0.00257)	-0.00046 (0.0023)
Conjugate Linear Regression			
Method	$d = 11$	$d = 101$	$d = 1001$
true value	-269.73904	-347.81384	-320.59267
mean field gaussian	-271.18867 (0.48871)	-377.48859 (1.99237)	-2096.65892 (15.65285)
standard	-269.73904 (0.00041)	-347.81354 (0.00239)	-321.87012 (0.83609)
ATAF	-269.73903 (0.00027)	-347.81391 (0.00234)	-321.86561 (0.4688)
SymClip	-269.73905 (0.00056)	-347.81312 (0.00791)	-377.06485 (3.65637)
proposed (gaussian, with LOFT)	-269.73924 (0.00038)	-347.81352 (0.0013)	-321.66793 (0.96678)
proposed (student, with LOFT)	-269.73885 (0.00037)	-347.81321 (0.00196)	-321.71383 (0.46365)
proposed (gaussian, no LOFT)	-269.73924 (0.00038)	-347.81352 (0.0013)	-321.66793 (0.96678)
proposed (student, no LOFT)	-269.73885 (0.00037)	-347.81321 (0.00196)	-321.71383 (0.46365)
SMC	-281.18175 (3.00131)	-595.63322 (22.78467)	-3480.17078 (123.3412)

TABLE 11. Evaluation of all methods in terms of ELBO and log marginal likelihood estimates (standard deviation in brackets) for $d' \in \{10, 100, 1000\}$.

Horseshoe Logistic Regression Model ($r = 64$) – Synthetic Data – ELBO			
Method	$d' = 10$	$d' = 100$	$d' = 1000$
mean field gaussian	-50.16087 (0.02565)	-78.82118 (0.03113)	-206.80469 (0.04076)
standard	-43.58686 (0.00193)	-56.82198 (1.10275)	-170.82029 (0.39773)
ATAF	-43.58192 (0.00146)	-56.6599 (0.01174)	-150.64962 (0.36023)
SymClip	-43.6015 (0.00149)	-56.63336 (0.01441)	-154.68972 (0.06192)
proposed (gaussian, with LOFT)	-43.57562 (0.00114)	-56.16784 (0.00936)	-145.28784 (0.06735)
proposed (student, with LOFT)	-43.57637 (0.00101)	-56.10268 (0.01114)	-105.29181 (0.07462)
proposed (gaussian, no LOFT)	-43.59333 (0.00204)	-56.1108 (0.00909)	-156.21152 (0.07304)
proposed (student, no LOFT)	-43.57314 (0.00116)	-56.0003 (0.01031)	-123.24537 (0.08508)
Horseshoe Logistic Regression Model ($r = 64$) – Synthetic Data – Log Marginal Likelihood Estimate			
Method	$d' = 10$	$d' = 100$	$d' = 1000$
mean field gaussian	-45.81527 (0.54777)	-68.21041 (1.24219)	-178.97184 (2.58527)
standard	-43.55468 (0.00181)	-54.70689 (0.33386)	-143.3784 (1.98397)
ATAF	-43.55316 (0.00466)	-54.73648 (0.58386)	-122.16614 (2.35816)
SymClip	-43.5537 (0.01553)	-54.90284 (0.13389)	-127.47038 (2.08928)
proposed (gaussian, with LOFT)	-43.55563 (0.00156)	-54.73608 (0.21571)	-116.7371 (2.77658)
proposed (student, with LOFT)	-43.55656 (0.00151)	-54.70299 (0.16654)	-81.45998 (2.62084)
proposed (gaussian, no LOFT)	-43.55392 (0.00389)	-54.72848 (0.23261)	-127.96218 (2.46497)
proposed (student, no LOFT)	-43.5535 (0.00213)	-54.69696 (0.12413)	-97.01509 (2.01398)
SMC	-72.15519 (0.60622)	-316.74614 (1.23563)	-2605.75083 (0.82943)
Horseshoe Logistic Regression Model ($r = 16$) – Synthetic Data – ELBO			
Method	$d' = 10$	$d' = 100$	$d' = 1000$
mean field gaussian	-50.16087 (0.02565)	-78.82118 (0.03113)	-206.80469 (0.04076)
standard	-43.59642 (0.00235)	-58.35805 (0.02742)	-172.75058 (0.0779)
ATAF	-43.60519 (0.00209)	-58.47138 (0.10144)	-151.93924 (0.17945)
SymClip	-43.71616 (0.00359)	-59.93733 (0.01882)	-171.2301 (0.07379)
proposed (gaussian, with LOFT)	-43.642 (0.00259)	-58.80727 (0.01738)	-166.96998 (0.06232)
proposed (student, with LOFT)	-43.61169 (0.00202)	-57.26398 (0.01502)	-129.22909 (0.08087)
proposed (gaussian, no LOFT)	-43.64326 (0.00271)	-58.78684 (0.01471)	-167.61975 (0.05924)
proposed (student, no LOFT)	-43.60367 (0.00203)	-57.25689 (0.01509)	-130.20364 (0.07451)
Horseshoe Logistic Regression Model ($r = 16$) – Synthetic Data – Log Marginal Likelihood Estimate			
Method	$d' = 10$	$d' = 100$	$d' = 1000$
mean field gaussian	-45.81527 (0.54777)	-68.21041 (1.24219)	-178.97184 (2.58527)
standard	-43.55501 (0.0045)	-55.21554 (0.26658)	-145.56326 (2.11553)
ATAF	-43.55648 (0.00472)	-55.3366 (0.18181)	-122.46094 (2.26795)
SymClip	-43.57685 (0.01127)	-56.1934 (0.27895)	-144.30236 (2.41617)
proposed (gaussian, with LOFT)	-43.56231 (0.01606)	-55.68322 (0.24981)	-140.06385 (1.82293)
proposed (student, with LOFT)	-43.55693 (0.00564)	-54.97434 (0.21206)	-101.48784 (2.69617)
proposed (gaussian, no LOFT)	-43.56263 (0.01568)	-55.6475 (0.36711)	-140.41891 (2.16415)
proposed (student, no LOFT)	-43.55214 (0.02036)	-54.93189 (0.27887)	-101.52184 (2.82329)
SMC	-72.15519 (0.60622)	-316.74614 (1.23563)	-2605.75083 (0.82943)

REFERENCES

- Uri Alon, Naama Barkai, Daniel A Notterman, Kurt Gish, Suzanne Ybarra, Daniel Mack, and Arnold J Levine. Broad patterns of gene expression revealed by clustering analysis of tumor and normal colon tissues probed by oligonucleotide arrays. *Proceedings of the National Academy of Sciences*, 96(12):6745–6750, 1999. [10](#)
- Daniel Andrade. Loft-stable training of normalizing flows for variational inference. In *The 6th Workshop on Tractable Probabilistic Modeling*, 2023. [2](#)
- Michael Arbel, Alex Matthews, and Arnaud Doucet. Annealed flow transport monte carlo. In *International Conference on Machine Learning*, pages 318–330. PMLR, 2021. [2](#), [9](#), [18](#)
- Lynton Ardizzone, Carsten Lüth, Jakob Kruse, Carsten Rother, and Ullrich Köthe. Guided image generation with conditional invertible neural networks. *arXiv preprint arXiv:1907.02392*, 2019. [2](#), [6](#), [7](#), [8](#)
- Jens Behrmann, Paul Vicol, Kuan-Chieh Wang, Roger Grosse, and Jörn-Henrik Jacobsen. Understanding and mitigating exploding inverses in invertible neural networks. In *International Conference on Artificial Intelligence and Statistics*, pages 1792–1800. PMLR, 2021. [2](#)
- David M Blei, Alp Kucukelbir, and Jon D McAuliffe. Variational inference: A review for statisticians. *Journal of the American statistical Association*, 112(518):859–877, 2017. [1](#), [4](#)
- James Brofos, Marylou Gabrié, Marcus A Brubaker, and Roy R Lederman. Adaptation of the independent metropolis-hastings sampler with normalizing flow proposals. In *International Conference on Artificial Intelligence and Statistics*, pages 5949–5986. PMLR, 2022. [17](#)
- Carlos M Carvalho, Nicholas G Polson, and James G Scott. The horseshoe estimator for sparse signals. *Biometrika*, 97(2):465–480, 2010. [9](#)
- Hugh Chipman, Edward I George, Robert E McCulloch, Merlise Clyde, Dean P Foster, and Robert A Stine. The practical implementation of bayesian model selection. *Lecture Notes-Monograph Series*, pages 65–134, 2001. [9](#)
- Chenguang Dai, Jeremy Heng, Pierre E Jacob, and Nick Whiteley. An invitation to sequential monte carlo samplers. *Journal of the American Statistical Association*, 117(539):1587–1600, 2022. [2](#), [9](#), [18](#)
- Akash Kumar Dhaka, Alejandro Catalina, Michael R Andersen, Måns Magnusson, Jonathan Huggins, and Aki Vehtari. Robust, accurate stochastic optimization for variational inference. *Advances in Neural Information Processing Systems*, 33:10961–10973, 2020. [12](#)
- Akash Kumar Dhaka, Alejandro Catalina, Manushi Welandawe, Michael R Andersen, Jonathan Huggins, and Aki Vehtari. Challenges and opportunities in high dimensional variational inference. *Advances in Neural Information Processing Systems*, 34:7787–7798, 2021. [1](#), [2](#)
- Laurent Dinh, Jascha Sohl-Dickstein, and Samy Bengio. Density estimation using real nvp. *arXiv preprint arXiv:1605.08803*, 2016. [4](#), [5](#), [8](#)
- Paul Hagemann and Sebastian Neumayer. Stabilizing invertible neural networks using mixture models. *Inverse Problems*, 37(8):085002, 2021. [2](#)
- Matthew D Hoffman, Andrew Gelman, et al. The no-u-turn sampler: adaptively setting path lengths in hamiltonian monte carlo. *J. Mach. Learn. Res.*, 15(1):1593–1623, 2014. [10](#), [18](#)

- Chin-Wei Huang, Laurent Dinh, and Aaron Courville. Augmented normalizing flows: Bridging the gap between generative flows and latent variable models. *arXiv preprint arXiv:2002.07101*, 2020. [5](#)
- Isao Ishikawa, Takeshi Teshima, Koichi Tojo, Kenta Oono, Masahiro Ikeda, and Masashi Sugiyama. Universal approximation property of invertible neural networks. *Journal of Machine Learning Research*, 24(287):1–68, 2023. [5](#)
- Priyank Jaini, Ivan Kobyzev, Yaoliang Yu, and Marcus Brubaker. Tails of lipschitz triangular flows. In *International Conference on Machine Learning*, pages 4673–4681. PMLR, 2020. [2](#), [7](#), [8](#)
- Ghassen Jerfel, Serena Wang, Clara Fannjiang, Katherine A Heller, Yian Ma, and Michael I Jordan. Variational refinement for importance sampling using the forward kullback-leibler divergence. *arXiv preprint arXiv:2106.15980*, 2021. [10](#)
- Diederik P Kingma and Jimmy Ba. Adam: A method for stochastic optimization. In *ICLR*, 2015. [9](#)
- Elizabeth Koehler, Elizabeth Brown, and Sebastien J-PA Haneuse. On the assessment of monte carlo error in simulation-based statistical analyses. *The American Statistician*, 63(2):155–162, 2009. [10](#)
- Frederic Koehler, Viraj Mehta, and Andrej Risteski. Representational aspects of depth and conditioning in normalizing flows. In *International Conference on Machine Learning*, pages 5628–5636. PMLR, 2021. [2](#), [5](#)
- Alp Kucukelbir, Dustin Tran, Rajesh Ranganath, Andrew Gelman, and David M Blei. Automatic differentiation variational inference. *Journal of machine learning research*, 2017. [9](#)
- Holden Lee, Chirag Pabbaraju, Anish Prasad Sevekari, and Andrej Risteski. Universal approximation using well-conditioned normalizing flows. *Advances in Neural Information Processing Systems*, 34:12700–12711, 2021. [5](#)
- Feynman Liang, Michael Mahoney, and Liam Hodgkinson. Fat-tailed variational inference with anisotropic tail adaptive flows. In *International Conference on Machine Learning*, pages 13257–13270. PMLR, 2022. [2](#), [8](#), [16](#)
- Alex Matthews, Michael Arbel, Danilo Jimenez Rezende, and Arnaud Doucet. Continual repeated annealed flow transport monte carlo. In *International Conference on Machine Learning*, pages 15196–15219. PMLR, 2022. [2](#)
- Radford M Neal. Annealed importance sampling. *Statistics and computing*, 11:125–139, 2001. [9](#), [18](#)
- Radford M Neal. Slice sampling. *The annals of statistics*, 31(3):705–767, 2003. [8](#)
- Radford M Neal et al. Mcmc using hamiltonian dynamics. *Handbook of markov chain monte carlo*, 2(11):2, 2011. [10](#)
- George Papamakarios, Eric Nalisnick, Danilo Jimenez Rezende, Shakir Mohamed, and Balaji Lakshminarayanan. Normalizing flows for probabilistic modeling and inference. *Journal of Machine Learning Research*, 22(57):1–64, 2021. [1](#), [4](#), [9](#)
- Adam Paszke, Sam Gross, Soumith Chintala, Gregory Chanan, Edward Yang, Zachary DeVito, Zeming Lin, Alban Desmaison, Luca Antiga, and Adam Lerer. Automatic differentiation in pytorch. 2017. [13](#)
- Du Phan, Neeraj Pradhan, and Martin Jankowiak. Composable effects for flexible and accelerated probabilistic programming in numpyro. *arXiv preprint arXiv:1912.11554*, 2019. [13](#)
- Rajesh Ranganath, Sean Gerrish, and David Blei. Black box variational inference. In *Artificial intelligence and statistics*, pages 814–822. PMLR, 2014. [3](#)

- Danilo Rezende and Shakir Mohamed. Variational inference with normalizing flows. In *International conference on machine learning*, pages 1530–1538. PMLR, 2015. [2](#), [12](#), [16](#)
- Geoffrey Roeder, Yuhuai Wu, and David K Duvenaud. Sticking the landing: Simple, lower-variance gradient estimators for variational inference. *Advances in Neural Information Processing Systems*, 30, 2017. [2](#), [4](#), [12](#), [16](#), [19](#)
- Antoine Salmona, Valentin De Bortoli, Julie Delon, and Agnès Desolneux. Can push-forward generative models fit multimodal distributions? *Advances in Neural Information Processing Systems*, 35:10766–10779, 2022. [2](#)
- Vincent Stimper, David Liu, Andrew Campbell, Vincent Berenz, Lukas Ryll, Bernhard Schölkopf, and José Miguel Hernández-Lobato. normflows: A PyTorch Package for Normalizing Flows. *arXiv preprint arXiv:2302.12014*, 2023. [13](#)
- Robert Tibshirani. Regression shrinkage and selection via the lasso. *Journal of the Royal Statistical Society. Series B (Methodological)*, pages 267–288, 1996. [17](#)
- Lorenz Vaitl, Kim A Nicoli, Shinichi Nakajima, and Pan Kessel. Gradients should stay on path: better estimators of the reverse-and forward kl divergence for normalizing flows. *Machine Learning: Science and Technology*, 3(4):045006, 2022. [1](#), [2](#), [4](#), [12](#), [16](#), [19](#)
- Steven Winter, Trevor Campbell, Lizhen Lin, Sanvesh Srivastava, and David B Dunson. Machine learning and the future of bayesian computation. *arXiv preprint arXiv:2304.11251*, 2023. [17](#)
- Cheng Zhang, Judith Bütepage, Hedvig Kjellström, and Stephan Mandt. Advances in variational inference. *IEEE transactions on pattern analysis and machine intelligence*, 41(8):2008–2026, 2018. [1](#)